MODELING ELECTROLYTE SOLUTIONS IN A STATISTICAL ASSOCIATING FLUID THEORY (SAFT) FRAMEWORK

A Thesis

by

MUAZ AHMED SELAM

Submitted to the Office of Graduate and Professional Studies of
Texas A&M University
in partial fulfillment of the requirements for the degree of

MASTER OF SCIENCE

Chair of Committee,	Ioannis Economou
Co-Chair of Committee,	Marcelo Castier
Committee Member,	Othmane Bouhali
Head of Department,	M. Nazmul Karim

July 2017

Major Subject: Chemical Engineering

ABSTRACT

SAFT-VR Mie is one of the most recent extensions of Statistical Associating Fluid Theory (SAFT). It is based on the Mie potential, which is a generalized form of the Lennard-Jones potential in which the exponents of the repulsive and attractive terms are allowed to vary from 12 and 6, respectively. In this thesis, the latest formulation of SAFT-VR Mie is implemented to accurately calculate densities and phase equilibria of both associating and non-associating fluid mixtures. The model is subsequently extended to mixtures with strongly dissociating electrolytes in water through the addition of a Born term to account for solvation effects and a Debye-Hückel term for long-range, electrostatic interactions. A single adjustable parameter is assigned to each ionic species (the cross dispersion energy between the ion and solvent) and is optimized against experimental data for electrolyte solution densities and mean ionic activity coefficients using a sequential Nelder-Mead algorithm with a parallel objective function evaluation.

Model correlations for the activity coefficients and liquid densities, as well as predictive calculations of vapor pressure, osmotic coefficients and mixed ion properties, show that the model's performance is comparable to that of other recent formulations for electrolyte solutions. Further improvement in a subsequent generation of the proposed equation of state will likely derive from a better description of dielectric phenomena, and adjustments to the parameter optimization strategy.

DEDICATION

To my parents for their unwavering and sincere concern for my well-being, the countless late-night conversations about work and spirituality and, like true software engineers, for always emphasizing the importance of backing up my files.

ACKNOWLEDGEMENTS

I am eminently grateful to Dr. Ioannis Economou and Dr. Marcelo Castier for granting me a Research Assistantship position – enabling me to complete both my Master's thesis and coursework in a conducive atmosphere. I am also thankful for their guidance, responsiveness and candid feedback throughout the course of my Master's research project, without which its successful completion would not have been possible. I would like to thank Dr. Othmane Bouhali for his meaningful input at both the thesis proposal and final thesis stages.

I am grateful to Dr. Othon Moultos for his very comprehensive, one-on-one FORTRAN tutorials during the first month of my work as a Research Assistant. The depth and breadth of topics covered and the very thoughtfully developed mini-assignments adequately prepared me in a short period for all of the programming necessary for thermodynamic modeling.

I would like to thank Dr. Luis Fernando Mercier Franco especially, with whom I communicated most frequently throughout the project. Often I would go to him with a single question, which would then rapidly evolve into a much deeper discussion – helping me better contextualize my work with broader discourse in applied thermodynamics.

CONTRIBUTORS AND FUNDING SOURCES

Contributors

This work was supervised by a thesis committee consisting of Professor Ioannis Economou and Professor Marcelo Castier of the Chemical Engineering Program, and Professor Othmane Bouhali of the Science Program.

The routines for SAFT-VR Mie for non-associating mixtures were developed by Dr. Luis Fernando Mercier Franco. The parameter fitting routines used in the project were developed previously by Professor Marcelo Castier. Dr. André Zuber provided experimental data files for parameter fitting.

All other work conducted for the thesis was completed by the student independently.

Funding Sources

This work was made possible by the National Priorities Research Program (NPRP) of Qatar National Research Fund under Grant Number 6-1157-2-471 and Texas A&M University at Qatar proof & seed program under Grant Number 482172-50580. The content of the work is solely the responsibility of the author and does not necessarily represent the official views of the Qatar National Research Fund (a member of Qatar Foundation).

NOMENCLATURE

A	Helmholtz free energy of system
a	Reduced/specific Helmholtz free energy; Characteristic ionic diameter
C	Mie potential pre-factor
d	Segment hard-sphere diameter
e	Elementary charge
F	Mayer function
f	Fugacity
g	Molar Gibbs' free energy; Kirkwood g-factor
g^{Mie}	Radial distribution function of reference Mie fluid
$\boldsymbol{I}$	Ionization potential; Association kernel
k	Boltzmann constant
M	Molar mass
m	Molality
m_s	Number of spherical segment per molecule
N	Number of molecules in system
N_A	Avogadro's number
N_s	Number of spherical segments in system
n	Number of moles

P	Pressure
P'	Probability that a molecule is involved in hydrogen bond
Q	Canonical partition function
R	Ideal gas constant
r	Intermolecular distance
r'	Born cavity radius
r^c	Diameter of association site
r^d	Distance between molecule's repulsive core and association site
S	Entropy of system
T	Absolute temperature
u	Intermolecular potential
V	Volume of system
v	Molar volume
X	Monomer fraction
x	Mole fraction
$x^{'}$	Mole fraction on ion-free basis
Z	Compressibility factor; Ion valence
z	Global composition of multiphase system; Molecular coordination number

Greek letters

α_0	Polarizability
γ	Activity coefficient; Angle between dipole moments

γ^m	Activity coefficient – molality basis
$\gamma_{\pm}^m$	Mean ionic activity coefficient – molality basis
Δ^{AB}	Association strength between generic sites A and B
ε	Minimum of intermolecular potential
ε_0	Permittivity of free space
ε_r	Relative permittivity
ε_∞	Permittivity at infinite frequency
θ	Bond angle
κ	Inverse Debye screening length
Λ	de Broglie wavelength
λ	Attractive/repulsive exponent in Mie potential
μ	Chemical potential
μ_0	Vacuum dipole moment
υ	Sum of ion valences in a given salt
ρ	Number density
σ	Segment diameter (as in Mie potential)
Φ	Osmotic coefficient
ϕ	Fugacity coefficient; Volume fraction
φ	Fraction of total system moles in a given phase

Abbreviations

NC	Index denotes number of components

NIONS	Index denotes number of ions
NP	Index denotes number of experimental data points
NSITES	Index denotes number of sites
NSOLV	Index denotes number of solvents

TABLE OF CONTENTS

Page

LIST OF FIGURES

Page

LIST OF TABLES

Page

1. INTRODUCTION

1.1. Background

Chemical Engineering design depends upon reliable property data. A quantitative representation of the volumetric/calorimetric properties and phase stability of pure components and mixtures is vital to modelling the performance of unit operations. Such a quantitative representation may take the form of tabulated data, diagrams, or mathematical models known as *equations of state*.

The prediction of fluid properties inductively using tabulated experimental data (or purely empirical models fitted against experimental data) may seem the most attractive and reliable. However, given the large number of multi-component mixtures that are of interest to engineering design, and the broad range of conditions at which they exist in various processes, the aspiration to rely solely on experimental data rapidly becomes impractical. Dependence on exhaustive experimental data also goes against our intuitive expectation that there is a certain wholeness or interconnectedness in the way systems behave – an idea that motivates the *Theory of Corresponding States* [1].

Thermodynamic properties may also be obtained from computer-based Molecular Dynamics Simulations – sometimes referred to as *computer* experiments – wherein molecular force-fields applied to an N-body system are integrated over time to calculate its trajectory [2]. While this can be a very useful tool in that it precludes the need for complex experimental setups, it also cannot be relied upon as our sole source of thermodynamic information because it is computationally expensive – often necessitating

the use of advanced computing resources. Even when such resources are available, many systems remain beyond reach.

Equations of state (EoS) are most often semi-empirical, incorporating insight gained from experimental data and molecular simulation to formulate a model fundamentally based in theory. EoS developed from the **Statistical Associating Fluid Theory (SAFT)** belong to a relatively new generation of models derived from statistical mechanics [3-6], and it is specifically **SAFT-VR Mie** (VR ≡ Variable Range) which is implemented in this project, and extended to systems with electrolytes [7]. This EoS models dispersion interactions with the generic Mie potential, which treats the energy of short-range attractive and repulsive interactions as proportional to $1/r^{\lambda_a}$ and $1/r^{\lambda_r}$ respectively, where r is the intermolecular distance and λ_a and λ_r are attractive and repulsive exponents which are allowed to be component-specific (hence, of variable range). In the case of the conventional Lennard-Jones potential, the attractive and repulsive exponents are 6 and 12, respectively.

Deriving an equation of state from statistical mechanics is essentially the process of arriving at a general expression for the canonical partition function of a fluid (Q), which is related to the Helmholtz free energy (A) as follows [8]:

$$A = -kT \ln Q\left(T, V, \underline{n}\right) \tag{1.1}$$

where k is the Boltzmann constant; T, V and $\underline{n}$ are the temperature, volume, and composition profile vector (in terms of number of moles of each component) respectively.

It might be perceived that, once one arrives at a reliable expression for the Helmholtz free energy as a function of temperature, volume and composition, all applied

thermodynamic calculations follow readily. Challenges do arise at the stage of implementation and applied calculations, but it is fair to say that much of the enabling work has already been done. This follows from the fact that the Helmholtz free energy function generates all other thermodynamic properties. One may begin from the general expression for the Helmholtz free energy as a function of temperature, volume and composition:

$$dA = -SdT - PdV + \sum_{i=1}^{NC} \mu_i dn_i \tag{1.2}$$

where S and P are the entropy and pressure of the system, while μ_i is the chemical potential of component *i*.

Given that the Helmholtz free energy function is an exact differential, visual inspection shows that the following relations hold true:

$$-\left(\frac{\partial A}{\partial T}\right)_{V,\underline{n}} = S \tag{1.3}$$

$$-\left(\frac{\partial A}{\partial V}\right)_{T,\underline{n}} = P \tag{1.4}$$

$$\left(\frac{\partial A}{\partial n_i}\right)_{T,\mathrm{V},n_{j\neq i}} = \mu_i \tag{1.5}$$

Having obtained expressions for pressure and chemical potential, one can already implement phase equilibrium calculations. To calculate other thermodynamic properties, further derivatives (including those of higher order) can be arrived at after some mathematical manipulation and the application of Maxwell relations.

One immediately begins to see the advantage of Helmholtz free energy equations of state like those originating from SAFT. All the thermodynamic information about a given system is implicit in its Helmholtz free energy function – allowing applied calculations to follow naturally. This is a departure from empirical activity coefficient models, which can calculate phase equilibria and calorimetric properties, but contain no information about the volumetric behavior of the system.

That is not to say that SAFT-VR Mie is purely theoretical. Component-specific molecular parameters that factor into the Helmholtz free energy function are commonly regressed against experimental data. Additionally, to ensure the accurate representation of mixture phase equilibria, empirically-determined cross-interaction parameters are introduced into the mixing rules for component parameters, and sometimes even made to be temperature-dependent (as in [9]).

SAFT-VR Mie is thus a compromise between a rigorously theoretical model, and one that is suitable for real engineering applications. The real advantage of SAFT lies in its versatility. A single model can adequately predict properties of fluids of varying complexity. Because the energy contributions of different classes of intermolecular interactions are treated as additive, the model can readily be extended to systems with electrolytes by adding a coulombic term. The project seeks to extend the SAFT-VR Mie equation of state to electrolyte systems along these very lines.

1.2. Engineering Motivation

Electrolyte solutions tend to reside at the periphery of our conception of multi-component mixtures which are relevant to industrial processes. However, the

thermodynamics of electrolyte solutions is eminently applicable to hydrocarbon production in the context of, for example, modeling salt precipitation in drilling muds and the production of natural gas from aquifers where natural gas is in equilibrium with brines [10].

An equation of state which can reliably predict properties of aqueous mixtures containing electrolytes is also essential to, most notably, the design of desalination plants where vapor-liquid equilibria (in the case of thermal desalination) and osmotic pressure (in the case of reverse osmosis) calculations are central to controlling the performance of the process. Even more generally so, equipment sizing for such processes necessitates reliable data for calorimetric and volumetric properties. In this sense, information about the phase equilibria of electrolyte solutions is critical to water security.

1.3. Objectives

The aim of this project is to develop an extension of the SAFT-VR Mie equation of state to systems with electrolytes, and implement it to calculate volumetric behavior and phase equilibria of systems consisting of water and strongly dissociating ions. The various objectives associated with this aim are delineated below:

1. Implement the SAFT-VR Mie equation of state for spherical, non-spherical, non-associating and associating mixtures – verifying and reproducing vapor-liquid equilibrium and density data reported in the literature for the same model;
2. Implement an ion-based (as opposed to salt-based) model for the Helmholtz free energy contribution due to solvation effects and electrostatic interactions between ions;

3. Implement a suitable optimization strategy for the evaluation of model parameters;
4. Calculate densities, mean ionic activity coefficients, vapor pressures and osmotic coefficients for systems consisting of water and strongly dissociating salts.

2. LITERATURE REVIEW

2.1. Statistical Associating Fluid Theory (SAFT)

All SAFT models are developed as perturbation expansions of the Helmholtz free energy. This is also true for the Electrolattice [11] and Q-Electrolattice [12] models, which have been developed for systems with ionic interactions and also exist as expansions of Helmholtz free energy.

The defining feature of SAFT equations of state is their treatment of intermolecular interactions involving molecular association – an example of which is hydrogen bonding [13]. The Helmholtz free energy contribution from association applied to SAFT equations of state originates from a model by Wertheim, known as Wertheim's TPT1 (First Order Thermodynamic Perturbation Theory) which makes the following assumptions [3]:

a) Only a single molecule may bond at a given site;
b) A site on a given molecule may bond only with another single site on another molecule;
c) Double bonding between molecules is impermissible.

The model was extended to hypothetical molecules with spherical cores and bonding sites of a specific geometry relative to the center – resulting in the following expression for Helmholtz free energy [3], which is a summation over the total number of associating sites on the molecule:

$$\frac{A-A_0}{NkT} = \sum_{i}^{NSITES}\left(\ln X_i - \frac{X_i}{2} + \frac{1}{2}\right) \tag{2.1}$$

where X_i is the fraction of molecules not bonded at site *i*, *N* is the number of molecules, and A_0 is the Helmholtz free energy of the reference system. The elegance of Wertheim's theory is that it can be extended to non-spherical molecules (such as long-chain alkanes) by allowing site-site interactions to become very large [13] – resulting in a separate "chain" contribution to the Helmholtz free energy. By including an additional term for weaker interactions between chains (A_{seg}^{res}), one obtains a complete equation for the residual Helmholtz free energy of the system [13]:

$$A^{res} = A_{seg}^{res} + A_{chain}^{res} + A_{assoc}^{res} \tag{2.2}$$

Weaker dispersive interactions between segments were first modeled using a square-well potential [3].

2.2. SAFT-VR Mie

SAFT-VR Mie is a relatively recent equation of state, though it has many predecessors in the SAFT family [3-6]. It models dispersive interactions using the generic Mie potential, the parameters of which are allowed to be component-specific. The expression for the Mie potential is as follows:

$$u^{Mie}(r) = C\varepsilon\left[\left(\frac{\sigma}{r}\right)^{\lambda_r} - \left(\frac{\sigma}{r}\right)^{\lambda_a}\right] \tag{2.3}$$

where

$$C = \frac{\lambda_r}{\lambda_r - \lambda_a}\left(\frac{\lambda_r}{\lambda_a}\right)^{\frac{\lambda_a}{\lambda_r - \lambda_a}} \tag{2.4}$$

In these expressions, λ_a and λ_r are the attractive and repulsive exponents, respectively. σ is referred to as the segment diameter, and is the intermolecular distance at which the Mie potential assumes a value of zero. The minimum value for the potential of interaction is $-\varepsilon$. These four parameters are taken to be molecule (i.e. component) specific. Figure 1 provides a representative plot of this potential.

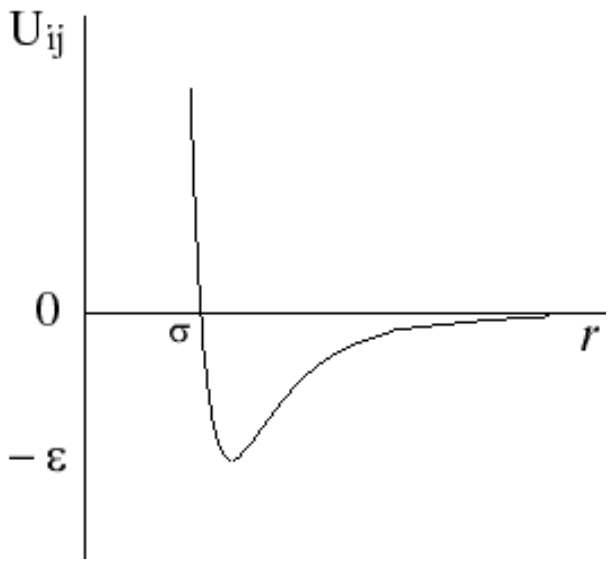

Figure 1: Representative graph of Mie potential

Much of the additional effort in developing this equation of state involves arriving at an approximation of the radial distribution function (RDF) which is consistent with the Mie potential. This new RDF changes not only the evaluation of energy due to dispersive

interactions, but also the evaluation of the chain and association terms – ensuring that the equation of state is internally consistent.

2.3. Non-Associating Pure Components

According to the SAFT-VR Mie formalism, the reduced Helmholtz free energy per molecular segment for a pure component system $a=(A/N_s kT)$ is given by [7]:

$$a = a^{IDEAL} + a^{MONO} + a^{CHAIN} + a^{ASSOC} \tag{2.5}$$

$$a^{IDEAL} = \ln(\rho\Lambda^3) - 1 \tag{2.6}$$

where Λ^3 is the de Broglie volume, and ρ is the number density. N_s is the number of monomer segments, and is given by:

$$N_s = m_s N \tag{2.7}$$

where m_s is the molecular chain length, and is typically determined by the regression of experimental data.

The monomer contribution, which represents dispersive interactions, is expressed as a perturbation expansion in temperature (with $\beta=1/kT$):

$$a^M = m_s(a^{HS} + \beta a_1 + \beta^2 a_2 + \beta^3 a_3) \tag{2.8}$$

This mathematical treatment, which is based on Barker-Henderson perturbation theory, expresses the dispersive contribution to the Helmholtz free energy as perturbations on a hard sphere reference system. Intuitively, a system of hard spheres may be likened to billiard balls moving about on a table. In this framework, the molecules do not interact with one another except at contact – where there is infinite repulsion. The equation of

state used to describe this hard sphere reference was first proposed by Carnahan and Starling [14].

The first two subsequent perturbation terms on the hard sphere reference are evaluated as integrals involving the Mie potential and hard sphere radial distribution function. The methodology to evaluate these integrals (including assumptions and approximations), as well as their final expressions may be found in the work by Laffite et al. [7]. Finally, the third perturbation term was developed numerically (using Monte Carlo simulation data).

The chain contribution to the Helmholtz free energy is expressed as follows:

$$a^{CHAIN} = -(m_s - 1)\ln g^{Mie}(\sigma) \tag{2.9}$$

where $g^{Mie}(\sigma)$ is the radial distribution function of the reference Mie fluid, which is a function of σ, the inter-particle distance at which the Mie potential is zero. This expression is based on the mathematical formulation for associating molecules – which models associating sites decorated on the molecule as square-well potentials, and are specified as non-zero in the range of σ to $\lambda\sigma$ (in terms of intermolecular distance). In the special case of chain-forming association, this square-well potential to describe this associating site is assigned an attractive potential (ε) of $-\infty$, and a λ value of 1. The main challenge is generating an approximation for the radial distribution function of the reference Mie fluid. This is discussed fully by Laffite et al. [7].

2.4. Non-Associating Mixtures

An additional degree of complexity emerges when extending the model, up until now presented only for pure fluids, to non-associating mixtures. This entails the

application mixing rules in order to calculate composition-based averages of each of the Helmholtz free energy contributions. For example, the first order perturbation coefficient in equation (2.8) is now expressed as follows:

$$a_1 = \sum_{i=1}^{NC}\sum_{j=1}^{NC} x_{s,i} x_{s,j} a_{1,ij} \tag{2.10}$$

where x_s is the is the segment mole fraction; i and j are component indices. The value for a_1 is calculated from $a_{1,ij}$, which is a two-dimensional matrix. This matrix is built by evaluating a_1 recursively for all combinations of pair-wise averaged equation of state parameters based on common combining rules. These combining rules are presented below for each of the SAFT-VR Mie parameters:

$$\sigma_{ij} = \frac{\sigma_{ii} + \sigma_{jj}}{2} \tag{2.11}$$

$$\lambda_{k,ij} - 3 = \sqrt{(\lambda_{k,ii} - 3)(\lambda_{k,\mathrm{jj}} - 3)}, k = a, r \tag{2.12}$$

$$\varepsilon_{ij} = \frac{\sqrt{\sigma_{ii}^3 \sigma_{jj}^3}}{\sigma_{ij}^3} \sqrt{\varepsilon_{ii}\varepsilon_{jj}} \tag{2.13}$$

2.5. Associating Mixtures

The expression for the association contribution to the Helmholtz free energy was presented for pure components. For mixtures, it is as follows [3]:

$$\frac{A^{ASSOC}}{kT} = \sum_{i}^{NC} N_i \sum_{A_i}^{NSITES} \left(\ln X_{A_i} - \frac{1}{2} X_{A_i} + \frac{1}{2} \right) \tag{2.14}$$

where *A* is the bonding site index and *i* is a component index. Non-bonded site fractions can be found by solving a system of non-linear equations.

$$X_{A_i} = \frac{1}{1+(1/V)\sum_{j}^{NC} N_j \sum_{B_j}^{NSITES} X_{B_j} \Delta^{A_i B_j}} \tag{2.15}$$

Again, *A* and *B* are site indices, while *i* and *j* are component indices. $\Delta^{A_i B_j}$ (association strength) is a function of the radial distribution function (RDF) of the Mie fluid and the depth of the association energy well. For a pure fluid, it is expressed as follows:

$$\Delta^{AB} = F^{AB} K^{AB} I \tag{2.16}$$

Here, F^{AB} is the Mayer function which is expressed as:

$$F^{AB} = \exp(-\varepsilon_{AB} / kT) \tag{2.17}$$

ε_{AB} represents the depth of the square well potential used to describe the association site. K^{AB} is referred to as the bonding volume and is meant to account for the geometric nature of a molecule's association site. In SAFT-VR Mie, it is treated as an adjustable parameter. Finally, I is referred to as the association kernel, and is evaluated as follows:

$$I = \frac{4\pi}{24(r^d)^2 \sigma^3} \int_{2r^d - r^c}^{2r^d + r^c} g^{Mie}(r)(2r^d + r^c - r)^2 (2r^c - 2r^d + r)^2 r dr \tag{2.18}$$

where r^c and r^d are geometric parameters which describe the association site. r^c is the diameter of the association site and r^d is the distance between the center of the spherical segment's repulsive core and the center of the association site (these parameters can be visualized on Figure 2). The approach used by Dufal et al. [9] is to solve for the radial distribution function of the Mie fluid using a numerical solution of the Ornstein-Zernike equation with the Reduced Hypernetted Chain (RHNC) closure. The association kernel is then evaluated numerically for various conditions and fitted to a polynomial function in

terms of reduced density, reduced temperature, and repulsive exponent in the Mie potential. Figure 2 presents a visual representation of the 4-site model used for water in SAFT-VR Mie, reproduced from [9].

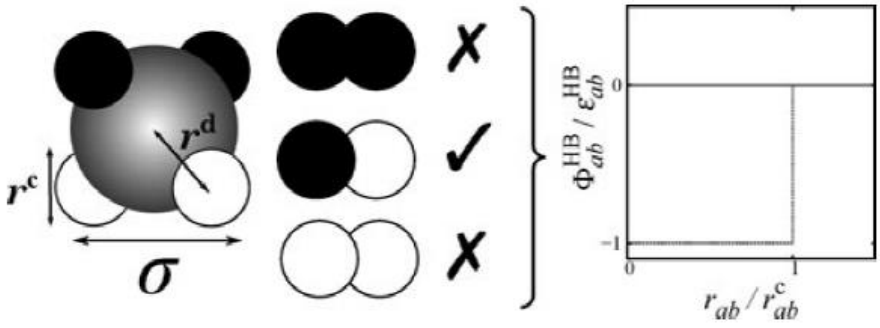

Figure 2: 4-site association model for water [9]

To calculate the association contribution to pressure and chemical potential, one can use the expression derived by Michelsen and Hendriks [15], which precludes the need to calculate derivatives of the monomer fraction. However, for properties involving higher order derivatives of the Helmholtz free energy (such as isothermal compressibility), higher order derivatives of the monomer fractions with volume and number of moles are evaluated as an iterative solution to the system of non-linear equations which emerge from taking the derivative of (2.15).

2.6. Contribution of Solvation Effects and Electrostatic Interactions to the Helmholtz Free Energy

Solvation Effects

Explicitly accounting for solvation effects using the Born equation ensures that the model can reliably calculate energies of solvation. The Born equation follows from integrating the electrostatic interactions between ion and the solvent from the surface of the ion to infinity [16]. The expression for the Helmholtz free energy contribution due to the solvation of one mole of ions is [16]:

$$\Delta A^{Born} = \frac{Z_i^2 e^2 N_A}{8\pi\varepsilon_0 r'_i}\left(\frac{1}{\varepsilon_r} - 1\right) \tag{2.19}$$

In this equation, Z_i is the charge on ion *i*, e is the elementary charge constant, N_A is Avogadro's number, ε_0 is the permittivity of free space, ε_r is the relative permittivity of the solvent and $r_i^{'}$ is the radius of the cavity occupied by ion *i* in the solvent.

Electrostatic Interactions

The contribution to the Helmholtz free energy due to electrostatic interactions can be modeled using the Debye-Hückel model or, alternatively, an expression based on the Mean Spherical Approximation (MSA) [16]. Maribo-Mogensen et al. [17] conducted a comparative study on the two models and concluded that the numerical complexity of the MSA expression was not justified by any improved performance; rather, the reliability of results is much more sensitive to the dielectric constant. They then opt to implement the Debye-Hückel model in conjunction with the Cubic Plus Association (CPA) equation of

state, with dielectric constants calculated using the method presented in [18, 19]. Details of both the MSA expression and Debye-Hückel model are presented below.

Mean Spherical Approximation (MSA)

The Mean Spherical Approximation (MSA) is a closure for the Ornstein-Zernike integral equation, which once applied in conjunction with a function for the intermolecular interactions of interest (in this case, Coulombic interactions), yields an expression for the radial distribution function (RDF) [8] which can subsequently be used to derive the expression for the canonical partition function and, by extension, the Helmholtz free energy of the system. The expression for the electrostatic contribution to the Helmholtz free energy from MSA is as follows [16]:

$$A^E = -\frac{Ve^2}{4\pi\varepsilon_r\varepsilon_0}\left(\Gamma\sum_i^{NIONS}\frac{\rho_i Z_i^2}{1+\Gamma a_i}+\frac{\pi}{2\Theta}\Omega P_n^2\right)+\frac{V\Gamma}{3\pi}kT \tag{2.20}$$

Here, ρ_i is the number density of component *i* and a_i is the hard sphere diameter of ion *i*. The terms in the equation are further expanded below:

$$\Omega = 1+\frac{\pi}{2\Theta}\sum_i^{NIONS}\frac{\rho_i a_i^3}{1+\Gamma a_i} \tag{2.21}$$

$$P_n = \frac{1}{\Omega}\sum_i^{NIONS}\frac{\rho_i a_i z_i}{1+\Gamma a_i} \tag{2.22}$$

$$\Theta = 1-\frac{\pi}{6}\sum_i^{NIONS}\rho_i a_i^3 \tag{2.23}$$

$$\Gamma = \frac{e}{2\sqrt{\varepsilon_r\varepsilon_0 kT}}\sum_i\rho_i\left(\left(Z_i-\frac{\pi a_i^2 P_n}{2\Theta}\right)/\left(1+\Gamma a_i\right)\right)^2 \tag{2.24}$$

Equations (2.21) and (2.22) couple ion charge with ion size, equation (2.23) relates the ion packing fraction, and equation (2.24) is the MSA screening parameter and is implicit (and therefore must be evaluated iteratively) [20].

The Debye-Hückel Equation

In order to calculate the radial distribution function (RDF) of ions in a dielectric medium, the Debye-Hückel approach solves Poisson's equation (for the charge density around an ion) while simultaneously assuming that the distribution of ions follows the Boltzmann distribution [16]. The expression for the Helmholtz free energy contribution due to electrostatic interactions is as follows [16]:

$$\frac{A^{elec}}{N_A kT} = -\frac{1}{3}\sum_{i}^{NIONS} x_i Z_i^2 s\kappa\chi\left(\kappa a_i\right) \tag{2.25}$$

where x_i is the mole fraction of ion *i*, κ is the inverse Debye screening length and a_i is its characteristic diameter. The terms in the equation are further expanded below:

$$s = \frac{e^2}{4\pi\varepsilon_0\varepsilon_r kT} \tag{2.26}$$

$$\kappa = \frac{e^2 N_A}{\varepsilon_0\varepsilon_r kT}\frac{\sum_{i}^{NIONS}\left(N_i Z_i\right)^2}{V} \tag{2.27}$$

$$x = \kappa a_i \tag{2.28}$$

$$\chi\left(x\right) = \frac{3}{x^3}\left(\frac{3}{2} + \ln\left(1+x\right) - 2\left(1+x\right) + \frac{1}{2}\left(1+x\right)^2\right) \tag{2.29}$$

2.7. Estimation of Solvent Dielectric Constant

The dielectric constant (or relative permittivity) is a measure of the polarizability of a given solvent; solvents with higher relative permittivity reduce electrostatic interactions between ions to a greater extent [16] – thereby "shielding" free ions from other ions in solution. This explains why salts require a polar solvent in order to dissociate – overcoming the strong electrostatic forces between cations and anions [16].

Relative permittivity (ε_r) is dimensionless and is defined as follows [16]:

$$\varepsilon_r = \frac{\varepsilon}{\varepsilon_0} \tag{2.30}$$

where ε is the permittivity of the solvent medium and ε_0 is the permittivity of free space. Reliable data for the relative permittivity is essential to model electrostatic interactions. Since the Born contribution is essentially a measure of energy due to the effect of solvation, it is unsurprising that the relative permittivity factors into the Born equation. Relative permittivity also factors into the Coulomb's law equation for electrostatic force because it has an attenuating effect on electrostatic interactions, and, by extension, the Debye-Hückel/MSA contribution to the Helmholtz free energy.

In the most general case, the dielectric constant of a solvent depends on temperature, volume, and ion concentration in the solvent. This suggests that the equation of state will be most successful at calculating properties over a broad range of conditions (including high salt concentrations) if the model for the dielectric constant makes allowance for such dependencies.

In a recent version of SAFT-VR Mie to which an MSA term has been added to model electrolytes [21], the dielectric constant is calculated from an empirical correlation previously proposed by the same group in conjunction with a SAFT-VR + MSA model [20]. The correlation is as follows:

$$\varepsilon_r = 1 + \rho_{solv} d \tag{2.31}$$

where ε_r is the dielectric constant, ρ_{solv} is the number density of the solvent, and d is a temperature-dependent solvent parameter evaluated as follows:

$$d = d_v \left(\frac{d_t}{T} - 1 \right) \tag{2.32}$$

in which d_v and d_t are solvent-dependent empirical parameters. In this formulation, the dielectric constant depends on temperature and solvent volume, but not on composition. In the case of mixed solvents, the following combining rule is applied to the dielectric constants of unlike solvent species:

$$d_{ij} = \frac{d_{ii} + d_{jj}}{2} \tag{2.33}$$

The dielectric constant for the mixed solvent is subsequently evaluated as a compositional average over all of the solvent species on an ion-free basis, according to the following mixing rule:

$$d = \sum_{i=1}^{NSOLV} \sum_{j=1}^{NSOLV} x_i' x_j' d_{ij} \tag{2.34}$$

Here, x' refers to solvent mole fractions on an ion-free basis. Alternatively, a very rigorous model has been developed by Maribo-Mogensen et al. [18, 19] which utilizes an

equation of state to model the dielectric properties of a given solvent – from which the temperature, volume and composition dependence of the dielectric constant naturally emerge. The operative equation is as follows [19]:

$$\frac{(2\varepsilon_r + \varepsilon_\infty)(\varepsilon_r - \varepsilon_\infty)}{\varepsilon_r(\varepsilon_\infty + 2)^2} = \frac{N_A}{9\varepsilon_0 kTv} \sum_i^{NSOLV} x_i g_i {\mu_{0,i}}^2 \tag{2.35}$$

where ε_∞ is the permittivity at infinite frequency, $\mu_{0,i}$ is the vacuum dipole moment of component *i*, v is the molar volume and g_i is the Kirkwood g-factor of component *i*. It is essentially the calculation of this g-factor which is non-trivial, and the model proposed by Maribo-Mogensen et al. utilizes ideas from association theory to quantify it. The final expression for the Kirkwood g-factor is:

$$g_i = 1 + \sum_j^{NSOLV} \frac{z_{ij} P_{ij}^{'} \cos\gamma_{ij}}{P_i^{'} \cos\theta_{ij} + 1} \frac{\mu_{0,j}}{\mu_{0,i}} \tag{2.36}$$

where z_{ij}, γ_{ij} and θ_{ij} are parameters related to the geometry of the dipole interaction between components *i* and *j*. $P_{ij}^{'}$ and $P_i^{'}$ are related to the monomer fractions of the components in that they represent probabilities that a molecule is involved in a hydrogen bond. Specifically:

$$P_{ij}^{'} = \sum_{B_j}^{NSITES} P_{A_i B_j}^{'} = 1 - X_{A_i} \tag{2.37}$$

$$P_i^{'} = \sum_j^{NSOLV} P_{ij}^{'} \tag{2.38}$$

Finally, it is worth discussing the empirical correlation proposed by Zuber at al. [22] which is temperature and composition dependent and, for mixed solvents, volume dependent as well. The expression for the dielectric constant is as follows:

$$\varepsilon_r = \frac{\varepsilon_r^{mix}}{1+\sum_i^{nions}\left[x_i \sum_j^{NSOLV} \alpha_{i,j}\phi_j\right]} \tag{2.39}$$

where x_i is the mole fraction of ion *i*, $\alpha_{i,j}$ is an ion-specific parameter for ion *i* in solvent *j*. ϕ_j is the volume fraction of solvent *j*. ε_r^{mix} is the solvent mixture dielectric constant (ion-free basis) – having averaged each of the pure solvent dielectric constants over the volume fractions of each solvent.

$$\varepsilon_r^{mix} = \sum_s^{NSOLV} \phi_s \varepsilon_{r,s}^{pure} \tag{2.40}$$

Pure solvent dielectric constants (ε_r^{pure}) are treated as temperature-dependent only – evaluated using the following empirical correlation [23]:

$$\varepsilon_r^{pure} = d_1 + \frac{d_2}{T} + d_3 T + d_4 T^2 + d_5 T^3 \tag{2.41}$$

where d_1 - d_5 are solvent-specific adjustable parameters.

2.8. Existing Models for Electrolyte Solutions

There are a number of existing models and equations of state in the literature which make use of the ideas already discussed to describe the thermodynamic behavior of solutions with electrolytes. These models are outlined in Table 1.

Table 1: Existing models for electrolyte solutions

Model Description	Reference
Peng-Robinson + Born term + MSA	[24]
PC-SAFT + Debye-Hückel (ePC-SAFT)	[25]
Mattedi-Tavares-Castier (MTC) + Born term + MSA (Electrolattice)	[11, 12]
Soave-Redlich-Kwong + TPT1 Association + Born term + Debye-Hückel (e-CPA)	[26]
SAFT-VR Mie + Born Term + MSA (SAFT-VRE Mie)	[21]

These equations of state work by recognizing the dichotomy between short range (dispersive) and long-range (electrostatic) interactions and attempting to model the contributions of each separately. This is summarized by Prausnitz et al. [10]. Models for short-range interactions are based on the Lewis-Randall framework, in which the independent variables which describe the system are temperature T, volume V, and the mole numbers of *all* species n_i. On the other hand, models for the long-range, electrostatic contribution (such as MSA and Debye-Hückel) are derived from the McMillan-Mayer framework, where the independent variables are temperature T, volume V, the mole

number of *solute* species n_k and the chemical potential of the solvent μ_s. For ordinary electrolyte solutions with relatively low salt concentrations (such as those studied in this work), this inconsistency has a negligible effect, but must otherwise be resolved in the case of high salt molality and mixed solvent solutions. This is accomplished through the mathematical conversion of thermodynamic variables from one framework to the other [10], as discussed by Friedman [27], for example.

Excess Gibbs' energy models (also referred to as activity coefficient models) are a widely used alternative to the Helmholtz free energy equations of state discussed so far. While such models can be used to calculate phase equilibria and calorimetric properties of electrolyte solutions, they do not provide any information about the volumetric behavior of the system. These models treat the excess Gibbs' energy as a sum of contributions from both short-range and long-range interactions, with the long-range contribution typically described by a Debye-Hückel-type term [10]. Examples of such models that are widely used include that of Pitzer [28, 29] and the NRTL-SAC (Nonrandom Two-Liquid Segment Activity Coefficient) model extended to electrolytes [30].

3. METHODOLOGY

In order to accomplish the objectives delineated at the outset of this proposal, and taking into account our analysis of the relevant literature, the following decisions were made:

- The algorithm developed by Iglesias-Silva et al. [31] is implemented and used for multi-component phase equilibria calculations.
- An empirical correlation (2.41) [23] is used to capture the temperature dependence of the dielectric constant. Composition and volume dependence of the dielectric constant is neglected.
- The Debye-Hückel and Born equations are implemented to account for electrostatic interactions and solvation effects, respectively.
- We adopt the strategy of Eriksen et al. [21] for the evaluation of ion-specific parameters in the equation of state, with some modifications.
- We follow a parameter optimization strategy similar to that used by Zuber et al. [12] in the context of the Q-Electrolattice equation of state.
- Where appropriate, Mathematica® has been used to calculate derivatives, along with the open source Thermath package, which converts Mathematica® output into FORTRAN code.

The subsequent sections unpack these broad steps so as to trace the natural progression of project outcomes.

3.1. Implementation of SAFT-VR Mie for Associating and Non-Associating Pure Components

SAFT-VR Mie was implemented in a FORTRAN code, in terms of the mathematical formulation presented by Laffite et al. [7] for pure, non-associating fluids and that by Dufal et al. [9] for associating mixtures. One of the first challenges faced was the evaluation of the reference hard sphere diameter, expressed as follows:

$$d = \int_0^{\sigma} (1 - \exp(-\beta u^{Mie}(r)))dr \tag{3.1}$$

Because of the relative mathematical complexity of the Mie potential, this integral cannot be solved analytically. This is the only instance in the entire SAFT-VR Mie equation of state where a numerical method must be applied at the level of the equation of state itself (all other integrals and derivatives are either evaluated analytically, or mapped onto a polynomial and then implemented as an analytical function in the EoS code).

This integral was initially solved using a Monte Carlo integration technique, which was eventually replaced with a pre-existing routine using five-point Gaussian quadrature, which is computationally much more efficient for a large number of calls. The resulting calculations of the monomer term perturbation coefficients were verified against literature results [7]. It was deduced that, in the context of pure fluids, derivatives of the Helmholtz free energy with volume would be sufficient for density and vapor pressure calculations. For the monomer term, these derivatives were evaluated using Mathematica®, the resulting expressions of which were converted to FORTRAN code using the relevant Thermath package. These derivatives were verified numerically.

With respect to associating fluids, the formalism presented by Michelsen and Hendriks [15] precludes the need to evaluate derivatives of monomer fractions to calculate pressure, which instead is evaluated as follows:

$$\frac{P^{ASSOC}}{RT} = \frac{1}{2V}\left(-h + \sum_{i}^{NC}\sum_{j}^{NC} n_i n_j \sum_{A_i}^{NSITES}\sum_{B_j}^{NSITES} X_{A_i} X_{B_j} + \frac{\partial \Delta^{A_i B_j}}{\partial V} \right) \tag{3.2}$$

$$h = \sum_{i}^{NC} n_i \sum_{A_i}^{NSITES} \left(1 - X_{A_i}\right) \tag{3.3}$$

The only derivative that must be explicitly taken with volume is that of the Δ function for association. Based on the mathematical treatment of Dufal et al. [9], this function is evaluated as a polynomial in reduced density, making the derivative trivial.

Locating Volume Roots and the Calculation of Vapor-Liquid Equilibria

Since SAFT-VR Mie is an expansion in Helmholtz free energy, it is a natural function of temperature and volume. This means that the equation of state is volume input – pressure output. For many engineering applications, however, we require the model to be pressure input – volume output. A pressure input scheme is especially crucial to phase equilibria calculations, which involve optimization problems where one of the constraints is that the pressure in all the phases must be equal.

Many algorithms exist to locate volume roots for a given pressure, the most robust being that developed by Topliss [32]. In this project, however, a makeshift routine was written and utilized for root location based on a simple Newton's-type method – noting that the mechanism for root location in the Topliss routine ultimately uses a similar

technique to zero in on the root, but with a more robust algorithm to identify a viable initial guess.

For a given objective pressure P^{obj}, one guesses the liquid and vapor densities. Using the equation of state, the model pressure and derivative of pressure with volume are calculated, which are then used to guide the subsequent guesses for densities until satisfactory convergence is achieved. For both liquid and vapor phase roots, the operative equation to guide each subsequent guess is as follows:

$$\rho_{i+1} = \rho_i + \frac{P^{obj} - P(T, \rho_i)}{\frac{dP(T, \rho_i)}{d\rho}} \tag{3.4}$$

Of course, some care must be taken with initial guesses to ensure that they are not in the metastable or unstable region of the isotherm, or that they are too far away from the vicinity of the root where the isotherm is too steep – prohibiting convergence of the Newton's method.

The key test to verify our implementation of SAFT-VR Mie for pure fluids is through vapor pressure calculations, for which the equation of state parameters have been originally optimized. Good agreement with experimental data for vapor pressure indicates a correct implementation of the equation of state (though this is not the only method of verification employed in the project). The conditions for vapor-liquid equilibrium are that the temperature, pressure and chemical potential of all components are equal in all of the phases:

$$T^{\alpha} = T^{\beta} = ... = T^{\pi} \tag{3.5}$$

$$P^{\alpha} = P^{\beta} = ... = P^{\pi} \tag{3.6}$$

$$\mu_i^{\alpha} = \mu_i^{\beta} = ... = \mu_i^{\pi} \mid i = 1, NC \tag{3.7}$$

where π represents the total number of phases at equilibrium.

Since the equation of state is temperature input, satisfying the first condition is trivial. But the question arises as to how to satisfy the equality of pressures and chemical potentials. Mathematical manipulations on the equality of chemical potentials condition gives us some insight as to how this may be achieved. The chemical potential *for a pure fluid* (in terms of Helmholtz free energy) can be transformed as follows:

$$\mu = \left(\frac{\partial A}{\partial n}\right)_{T,V} = \left(\frac{\partial (na)}{\partial n}\right)_{T,V} = a + n\left(\frac{\partial a}{\partial n}\right)_{T,V}$$

$$da = \left(\frac{\partial a}{\partial T}\right)_{\rho} dT + \left(\frac{\partial a}{\partial \rho}\right)_{T} d\rho$$

$$\left(\frac{\partial a}{\partial n}\right)_{T,V} = \left(\frac{\partial a}{\partial \rho}\right)_{T}\left(\frac{\partial \rho}{\partial n}\right)_{T,V} = \left(\frac{\partial a}{\partial \rho}\right)_{T}\left(\frac{\partial \left(n/V\right)}{\partial n}\right)_{T,V} = \frac{1}{V}\left(\frac{\partial a}{\partial \rho}\right)_{T}$$

$$\Rightarrow \mu = a + \rho\left(\frac{\partial a}{\partial \rho}\right)_{T} \tag{3.8}$$

The density derivative can subsequently be transformed into that of volume, through the following steps:

$$\mu = a + \rho\left(\frac{\partial a}{\partial V}\right)_{T}\frac{dV}{d\rho} = a + \rho\left(\frac{\partial a}{\partial V}\right)_{T}\frac{-n}{\rho^2}$$

$$\Rightarrow \mu = a - \left(\frac{\partial A}{\partial V}\right)_{T}\frac{1}{\rho}$$

$$\Rightarrow \mu = a + Pv = g \tag{3.9}$$

This is the well-known result that the chemical potential of a pure substance is equal to its specific Gibbs' free energy. This result can be substituted into the equality of chemical potential condition for phase equilibrium:

$$\begin{aligned} &\mu^{\alpha} = \mu^{\beta} \\ &\Rightarrow a^{\alpha} + P^{sat} v^{\alpha} = a^{\beta} + P^{sat} v^{\beta} \\ &\Rightarrow \frac{a^{\alpha} - a^{\beta}}{v^{\beta} - v^{\alpha}} = P^{\alpha} = P^{\beta} = P^{sat} \end{aligned} \tag{3.10}$$

Further manipulations of equation (3.10) result in Maxwell's equal area rule:

$$\begin{aligned} &a^{\alpha} - a^{\beta} = \int_{a^{\alpha}}^{a^{\beta}} da = P^{sat}(v^{\alpha} - v^{\beta}) \\ &\Rightarrow \int_{v^{\alpha}}^{v^{\beta}} -P dv + \int -s dT = P^{sat}(v^{\alpha} - v^{\beta}) \end{aligned}$$

Since the integrals are over an isotherm, the second term vanishes and one is left with the mathematical expression for Maxwell's equal area rule:

$$\int_{v^{\beta}}^{v^{\alpha}} P dv = P^{sat}(v^{\alpha} - v^{\beta}) \tag{3.11}$$

An algorithm for the calculation of vapor pressures emerges naturally from (3.10). This is delineated as follows:

1. Guess a value for P^{sat}
2. Calculated the liquid and vapor roots for this guess
3. Calculated the new guess for P^{sat} from equation (3.10)
4. Repeat from (2) until sufficient convergence is achieved

Again, care must be taken that the initial guess for P^{sat} is such that it has both liquid and vapor roots with respect to the isotherm.

3.2. Implementation of SAFT-VR Mie for Associating and Non-Associating Mixtures

An existing implementation of SAFT-VR Mie for non-associating mixtures was extended to associating mixtures with a view to calculate densities and vapor-liquid equilibria for binary mixtures.

Volume and Composition Derivatives for Association Term

Central to the association term is the evaluation of the monomer fraction i.e. the fraction of segments of each species which do not participate in a hydrogen bond. The expression for the monomer fraction is reproduced here:

$$X_{A_i} = \frac{1}{1+(1/V)\sum_{j}^{NC} N_j \sum_{B_j}^{NSITES} X_{B_j} \Delta^{A_i B_j}} \tag{2.15}$$

It was stated before that the Michelsen-Hendriks approach precludes the need to calculate derivatives of the monomer fraction with volume or composition to calculate pressure or chemical potential. However, for the evaluation of higher order derivative properties (such as isothermal compressibility or the derivative of chemical potential with composition) one is compelled to evaluate these derivatives.

Equation (2.15) results in a system of $NC \times NSITES$ non-linear equations which must be solved iteratively. It then follows that, for the derivatives of X, one may differentiate equation (2.15) in its general form and solve for the *system of derivatives* as well. In this fashion, one will solve a single system of $NC \times NSITES$ equations to evaluate

the derivatives of all the monomer fractions with volume, and NC systems of $NC \times NSITES$ equations to solve for the derivatives of all the monomer fractions with number of moles of each component.

Here we show a representative formulation for the derivative of equation (2.15) with respect to the number of molecules of a single component (δ_{ij} is the Kronecker delta).

$$\left(\frac{\partial X_{A_i}}{\partial N_l}\right)_{T,P,N_{k\neq l}} = -X_{A_i}{}^2 \frac{1}{V}\left[\sum_{j=1}^{NC}\delta_{jl}\sum_{B_j}^{NSITES} X_{B_j}\Delta^{A_iB_j} + \sum_{j=1}^{NC} N_j \sum_{B_j}^{NSITES}\left(\frac{\partial X_{b_j}}{\partial N_l}\Delta^{A_iB_j} + X_{B_j}\frac{\partial \Delta^{A_iB_j}}{\partial N_l}\right)\right]$$

$$= -X_{A_i}{}^2 \frac{1}{V}\left[\sum_{B_l}^{NSITES} X_{B_l}\Delta^{A_iB_l} + \sum_{j=1}^{NC} N_j \sum_{B_j}^{NSITES}\left(\frac{\partial X_{b_j}}{\partial N_l}\Delta^{A_iB_j} + X_{B_j}\frac{\partial \Delta^{A_iB_j}}{\partial N_l}\right)\right]$$

$$\Rightarrow \left(\frac{\partial X_{A_i}}{\partial N_l}\right)_{T,P,N_{k\neq l}} = -X_{A_i}{}^2 \frac{1}{V}\left[\sum_{B_l}^{NSITES} X_{B_l}\Delta^{A_iB_l} + \sum_{j=1}^{NC} N_j \sum_{B_j}^{NSITES}\left(\frac{\partial X_{b_j}}{\partial N_l}\Delta^{A_iB_j} + X_{B_j}\frac{\partial \Delta^{A_iB_j}}{\partial N_l}\right)\right] \quad (3.12)$$

Vapor-Liquid Equilibria

To calculate the phase equilibria of binary mixtures, we employ the algebraic method developed by Iglesias-Silva et al. [31] for multi-component, multi-phase phase equilibria. We present a derivation of the operating equations for the specific case of binary, two-phase equilibrium from the equality of chemical potentials (employing high-level substitutions based on well-known thermodynamic relationships).

Starting from the equality of chemical potentials condition:

$$\mu_1^\alpha = \mu_1^\beta$$
$$\mu_2^\alpha = \mu_2^\beta$$
$$\Rightarrow \mu_1^\alpha - \mu_2^\alpha = \mu_1^\beta - \mu_2^\beta$$

$$\Rightarrow \left(\frac{dg}{dx_1}\right)_{T,P}^{\alpha} = \left(\frac{dg}{dx_1}\right)_{T,P}^{\beta} \quad (3.13)$$

This is identical to the limit of global phase stability for the two phase binary system, and is the first operating equation for the method proposed in reference [31]. For the second operating equation:

$$\begin{aligned} & g^{\alpha} = x_1^{\alpha}\mu_1^{\alpha} + x_2^{\alpha}\mu_2^{\alpha} \\ & \Rightarrow g^{\alpha} = x_1^{\alpha}\mu_1^{\alpha} + (1 - x_1^{\alpha})\mu_2^{\alpha} \\ & \Rightarrow g^{\alpha} = (\mu_1^{\alpha} - \mu_2^{\alpha})x_1^{\alpha} + \mu_2^{\alpha} \\ & \Rightarrow g^{\alpha} = \left(\frac{dg}{dx_1}\right)_{T,P}^{\alpha} x_1^{\alpha} + \mu_2^{\alpha} \end{aligned}$$

Also, by symmetry:

$$g^{\beta} = \left(\frac{dg}{dx_1}\right)_{T,P}^{\beta} x_1^{\beta} + \mu_2^{\beta}$$

The final form of the second operating equation is attained by substituting for μ_2^{β}:

$$\frac{g^{\beta} - g^{\alpha}}{x_1^{\beta} - x_1^{\alpha}} = \left(\frac{dg}{dx_1}\right)_{T,P}^{\alpha} = \left(\frac{dg}{dx_1}\right)_{T,P}^{\beta} \tag{3.14}$$

This formulation for phase equilibria is mathematically analogous to that derived for the pure fluids in equation (3.10). As result, the algorithm for calculating the equilibrium conditions follows a similar logic:

1. Specify pressure and temperature at equilibrium condition
2. Guess value for $\left(\frac{dg}{dx_1}\right)_{T,P}$
3. Find vapor and liquid composition roots for chosen $\left(\frac{dg}{dx_1}\right)_{T,P}$

- Find vapor and liquid volume root for given temperature, pressure and composition guess of each phase

4. Using equation (3.14), generate new guess for $\left(\frac{dg}{dx_1}\right)_{T,P}$
5. Repeat from (3) until sufficient convergence is achieved

This can be generalized to multicomponent, multiphase system – in which case one would implement an iterative routine to solve the system of non-linear, algebraic equations that would emerge from the generalized operative equations derived by Iglesias et al. [31]:

$$\left(\frac{\partial g}{\partial x_i}\right)^{\alpha}_{T,P,x_{k\neq i}} - \left(\frac{\partial g}{\partial x_i}\right)^{p}_{T,P,x_{k\neq i}} = 0 \,|\, i = 1,2,...,\mathrm{NC}-1 \text{ and } p\ \pi,...,\gamma,\beta = \quad (3.15)$$

$$\left(g^i - g^{\alpha}\right) - \sum_{j=1}^{NC-1}\left(x_j^i - x_j^{\alpha}\right)\left(\frac{\partial g}{\partial x_j}\right)^{\alpha}_{T,P,x_{k\neq j}} = 0 \,|\, i = \beta,\gamma,...,p-1 \quad (3.16)$$

$$z_i - \sum_{k=1}^{p} x_i^k \varphi^k = 0 \,|\, i = 1,2,...,NC-1 \quad (3.17)$$

The final expression is the overall component mass balance, where z_i is the global composition of component i and φ^k is the fraction of moles in phase k.

Verifying the Internal Consistency of the Equation of State Implementation

A useful verification step for the implementation of SAFT-VR Mie is to ensure that Euler's relation is satisfied, which would imply that the equation of state is internally consistent with respect to the calculation of pressures and chemical potentials. This is especially useful in the process of debugging because it provides significant insight into where potential problems are. Euler's relation is as follows:

$$g = a + Pv = \sum_{i}^{NC} x_i \mu_i \tag{3.18}$$

Figure 3 illustrates is the result for the verification of Euler's relation for SAFT-VR Mie + Debye-Hückel + Born equation for a solution of a hypothetical 1:2 salt and water, where the error plotted is the difference between the right and left hand sides of equation (3.18).

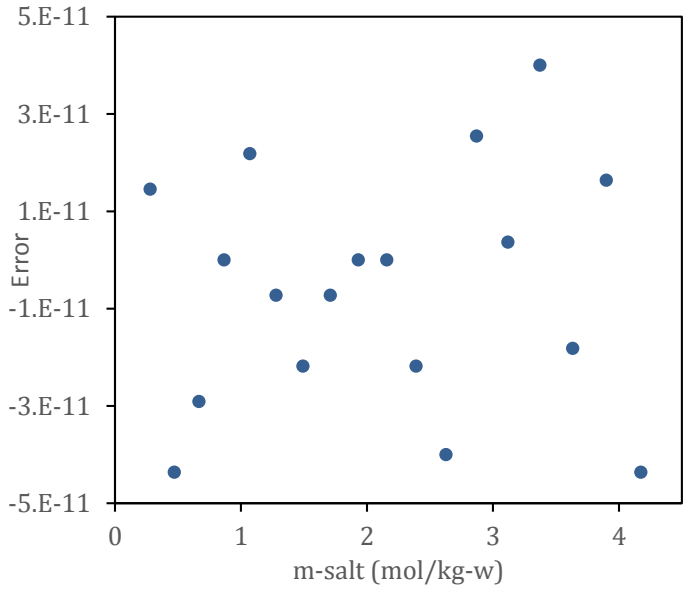

Figure 3: Error in Euler's relation in calculation by SAFT-VR Mie + electrostatic terms

The order of magnitude of this error reflects the allocated precision of the variables in the code. This is further validated by the fact that this error is statistically random.

A similar analysis was carried out for a representative associating mixture. The plot in Figure 4 shows the percentage absolute relative deviation (% ARD) between the

left and right hand sides of equation (3.18) for various compositions of a water + methanol mixture.

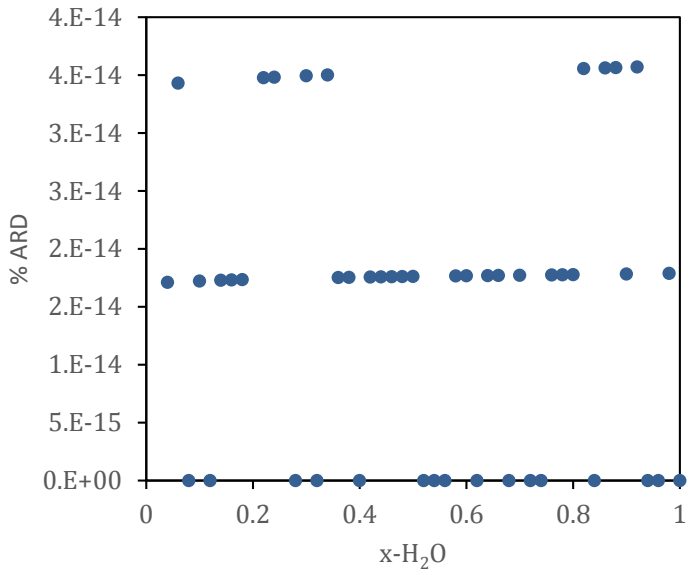

Figure 4: %ARD in Euler's relation as calculated by SAFT-VR Mie for a methanol + water mixture

From this analysis, we conclude that our implementation of the equation of state is internally consistent and that the volume and compositional derivatives of the Helmholtz free energy have been correctly evaluated.

3.3. Extension of SAFT-VR Mie to Electrolyte Solutions

The SAFT-VR Mie equation of state is extended to electrolyte solutions through the inclusion of the Born and Debye-Hückel terms to model solvation effects and long-range interactions, respectively. As before, this involves implementing expressions for

the Helmholtz free energy contribution of these terms and their derivatives with volume and composition. Here, we describe the methodology for ionic species parameter evaluation, and the formulae for thermodynamic property calculations for electrolyte solutions.

Parameter Evaluation Strategy

In an effort to minimize the number of adjustable parameters and to allow for the development of a meaningful, predictive equation of state, we adopt the methodology of Eriksen et al. [21] with respect to the specification of ion parameters. For instance, it is assumed that the ions behave as Lennard-Jones spheres – thereby eliminating the need to optimize the repulsive exponent or chain length. The Born cavity diameters are those reported by Rashin and Honig [33]. Segment diameters (σ) for each of the ionic species are taken to be the crystal radii (coordination VI) reported by Shannon [34]. We subsequently take the characteristic ionic diameter used in the Debye-Hückel expressions to be $5/6$ of the hard sphere diameter calculated by equation (3.1) for each of the ionic species. This accounts for effect of excluded volume, which is not treated explicitly by the Debye-Hückel formulation [17]. The ion-ion cross-dispersion energy parameters (both for identical and unlike ions) are calculated by equating the London dispersion interaction potential (explicit in terms of the electronic polarizability and ionization potential) with the attractive part of the Lennard-Jones potential. This is based on the approach for deriving the Hudson-McCoubrey combining rule, as presented by Haslam et al. [35]. We start from the operative expression for the London interaction potential:

$$\phi_{ij}^{London} = -\frac{3}{2}\frac{\alpha_{0,i}\alpha_{0,j}}{(4\pi\varepsilon_0)^2 r_{ij}^{\ 6}}\frac{I_i I_j}{(I_i + I_j)} \tag{3.19}$$

where $\alpha_{0,i}$ and I_i are the electronic polarizability and ionization potential of species *i*, respectively. This is equated to the attractive term of the Lennard-Jones potential, shown below:

$$\phi_{ij-attract}^{LJ} = -4\varepsilon_{ij}^{LJ}\left[\frac{\sigma_{ij}}{r_{ij}}\right]^6 \tag{3.20}$$

Having equated both expressions and solving for the dispersion energy parameters, one obtains the following expression:

$$\varepsilon_{ij} = \frac{3}{8}\frac{\alpha_{0,i}\alpha_{0,j}}{(4\pi\varepsilon_0)^2 \sigma_{ij}^6}\frac{I_i I_j}{(I_i + I_j)} \tag{3.21}$$

This approach differs from that of Eriksen et al. [21], which solves for the ion-ion dispersion parameters by equating *both the attractive and repulsive terms* of the Mie potential with the London dispersion interaction potential.

In this manner, the only adjustable parameter assigned to each ion is the cross dispersion energy parameter between the ion and the solvent. This has been optimized using the parameter optimization routine developed by Castier et al. [36] and applied successfully to the development of the Q-Electrolattice equation of state [12]. The in-house code uses a sequential Nelder-Mead algorithm with a parallel objective function evaluation – precluding the need to parallelize the code for the equation of state itself, while still allowing for the optimization program to be sped up with the help of parallel

computing resources. The objective function to be minimized is based on deviations from experimental data of the mean ionic activity coefficients and liquid densities [12]:

$$OF = \sum_{i=1}^{NP}\left(\frac{\gamma_{\pm}^{calc} - \gamma_{\pm}^{\exp}}{\gamma_{\pm}^{calc}}\right)^2 + \sum_{i=1}^{NP}\left(\frac{\rho_i^{calc} - \rho_i^{\exp}}{\rho_i^{calc}}\right)^2 \tag{3.22}$$

Thermodynamic Property Calculations of Electrolyte Solutions

Densities, mean ionic activity coefficients of ion pairs, osmotic coefficients, fugacity coefficients and vapor pressures were calculated for electrolyte solutions. The root-finding method discussed earlier was carried forward to electrolyte solutions for the calculation of densities.

Fugacity coefficients are obtained from the chemical potentials calculated by the equation of state as follows [24]:

$$\phi_i(T,P,\bar{n}) = \frac{1}{Z}\exp\left[\frac{\mu_i(T,P,\bar{n}) - \mu_i^{igm}(T,P,\bar{n})}{RT}\right] \tag{3.23}$$

where $\mu_i^{igm}(T,P,\bar{n})$ is the chemical potential of species i in the ideal gas mixture. The asymmetric activity coefficient of each ionic species on a molal basis can then be calculated as follows:

$$\gamma_i^m(T,P,\bar{n}) = \left(\frac{1}{1+\upsilon m M_{solvent}}\right)\left[\frac{\phi_i(T,P,\bar{n})}{\phi_i(T,P,\bar{n}=0)}\right] \tag{3.24}$$

where υ is the sum of the valences of each of the ions in the salt, m is the salt molality, $M_{solvent}$ is the molar mass of the solvent, and $\phi_i(T,P,\bar{n}=0)$ is the fugacity coefficient of species i at infinite dilution. The fugacity coefficient of the species at infinite dilution is

determined from the equation of state itself by determining the convergent fugacity coefficient at very low salt mole fractions. The mean ionic activity coefficient is subsequently evaluated as:

$$\gamma_{\pm}^{m} = \left[\left(\gamma_{+}^{m} \right)^{\upsilon^{+}} \left(\gamma_{-}^{m} \right)^{\upsilon^{-}} \right]^{1/\upsilon} \tag{3.25}$$

Finally, the osmotic coefficient is obtained from the following equation:

$$\Phi = -\frac{\ln(x_{solvent}\gamma_{solvent})}{\nu m M_{solvent}} \tag{3.26}$$

To simplify the calculation of vapor pressure, it is assumed that ion species are non-volatile. This means that it is sufficient for only the chemical potentials of water to be equal in the vapor and liquid phases. Based on this assumption, we have developed a short routine to calculate the pressure at which the fugacities of water in the liquid and vapor phases are equal, using the following relationships.

$$\begin{aligned} & f_w^{v} = f_w^{l} \\ & \Rightarrow \phi_w^{v}(T, P^{v}, \bar{n}) P^{v} = \phi_w^{l}(T, P^{l}, \bar{n}) P^{l} x_w^{l} \end{aligned} \tag{3.27}$$

At vapor-liquid equilibrium $P^{v} = P^{l} = P^{sat}$. Starting from an initial guess for P, one can readily calculate P^{sat} iteratively through successive substitution.

4. RESULTS AND DISCUSSION

4.1. SAFT-VR Mie

Having successfully implemented the SAFT-VR Mie equation of state for pure components (both associating and non-associating), as well as code developed for associating mixtures (which was incorporated to existing code for non-associating mixtures), we report here representative results for the phase equilibria of such systems and are compared with experimental data from the literature [37, 38], or model results generated by collaborators. Tables for pure component parameters used in conjunction with SAFT-VR Mie (as well as for calculating electrostatic contributions) are presented in the appendix.

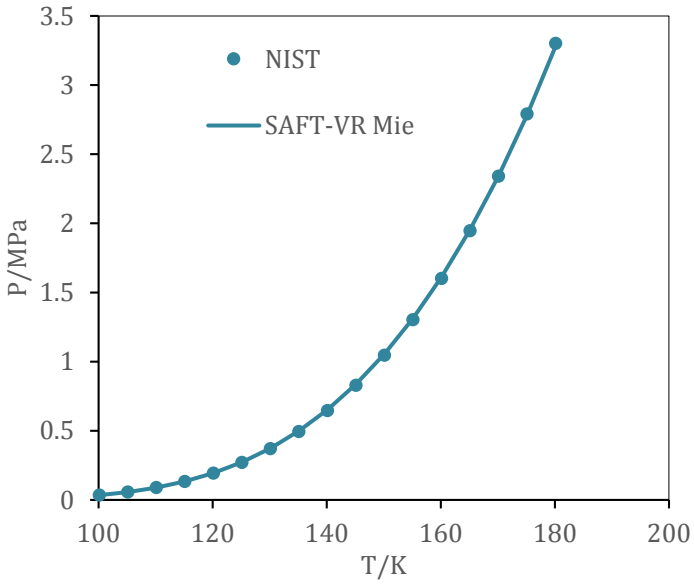

Figure 5: Methane vapor pressure curve (spherical molecule)

Methane is a spherical molecule $(m_s = 1)$ and is non-associating. Results shown in Figure 5 for the vapor pressure validate our implementation of the monomer term in SAFT-VR Mie. For the temperature range examined (100.15 K – 180.15 K), the %AARD between the experimental and model vapor pressures was 0.65%.

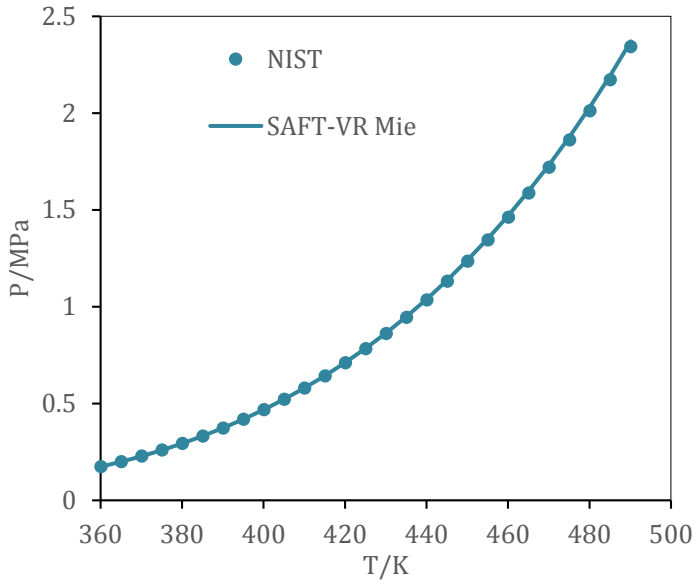

Figure 6: n-hexane vapor pressure curve (non-spherical molecule)

The vapor pressure plot shown in Figure 6 for n-hexane, which is non-spherical $(m_s = 2.1097)$ and non-associating, validates our implementation of the chain term in SAFT-VR Mie. For the temperature range examined (360.15 K – 490.15 K), the %AARD between the experimental and model vapor pressure was 0.51%.

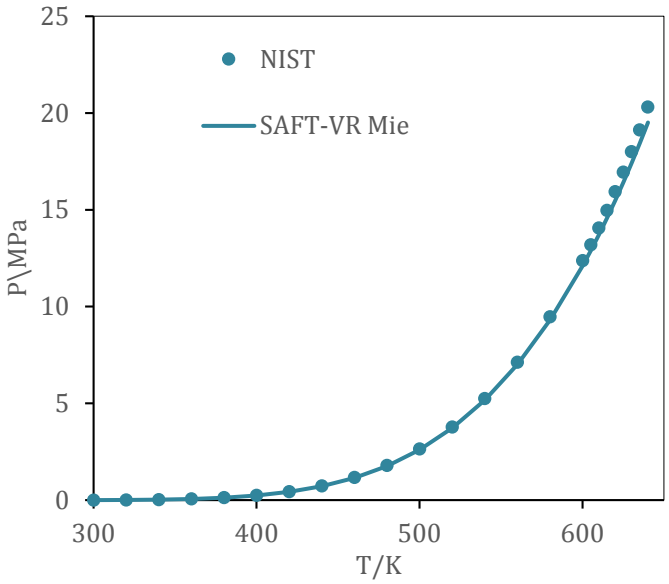

Figure 7: Water vapor pressure curve (associating, spherical molecule)

Figure 7 shows the vapor pressure for water, which is treated by SAFT-VR Mie as spherical and associating (with four association sites). Results validate our implementation of the association term in SAFT-VR Mie for pure components. For the temperature range presented (300.15 K – 640.15 K), the %AARD between experimental and model vapor pressure was 2.01%. In Figure 8, saturated liquid and vapor water densities are shown.

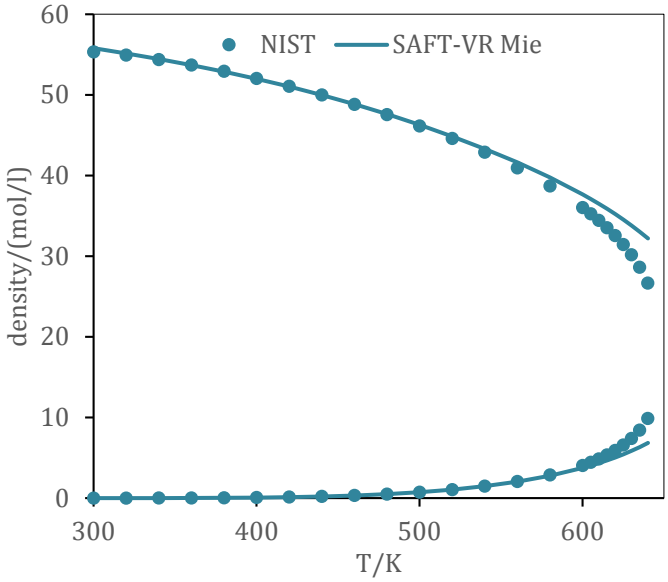

Figure 8: Saturated liquid and vapor densities for water

From this trend we infer that the equation of state over-predicts the critical temperature, which is the standard behavior of mean-field higher order EoS.

The following results for mixture vapor-liquid equilibria validate our implementation of SAFT-VR Mie for mixtures and the algorithm used to calculate phase equilibria.

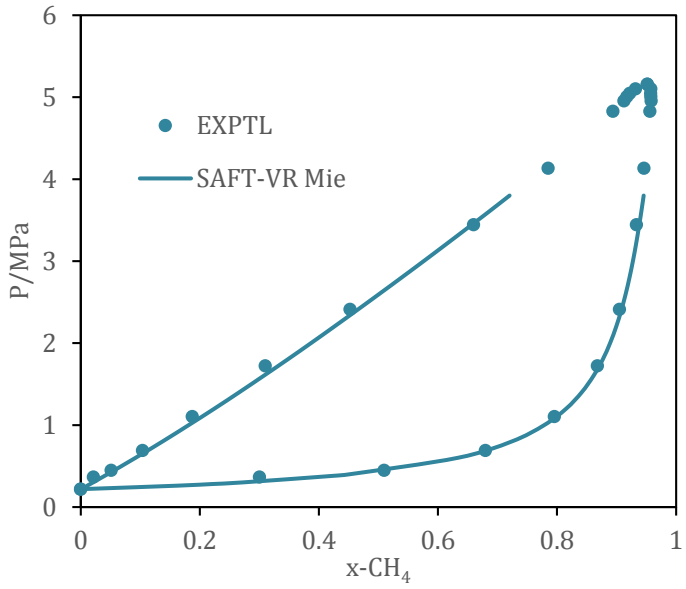

Figure 9: Methane + ethane VLE at 199.92 K superimposed with experimental data [38]

This VLE envelope for methane + ethane in Figure 9 was constructed without any binary interaction parameter. However, the chosen VLE routine fails to converge at pressures above 4 MPa, for which a more sophisticated VLE algorithm is needed. Such algorithms were recently developed in our research group at Texas A&M University at Qatar.

The subsequent VLE envelopes in Figure 10 for methanol + water (at 1 atm) show the results of a code-to-code comparison between the implementation of SAFT-VR Mie in this project and that of the collaborating group of Profs. Galindo and Jackson at Imperial College London, who are the original developers of SAFT-VR Mie.

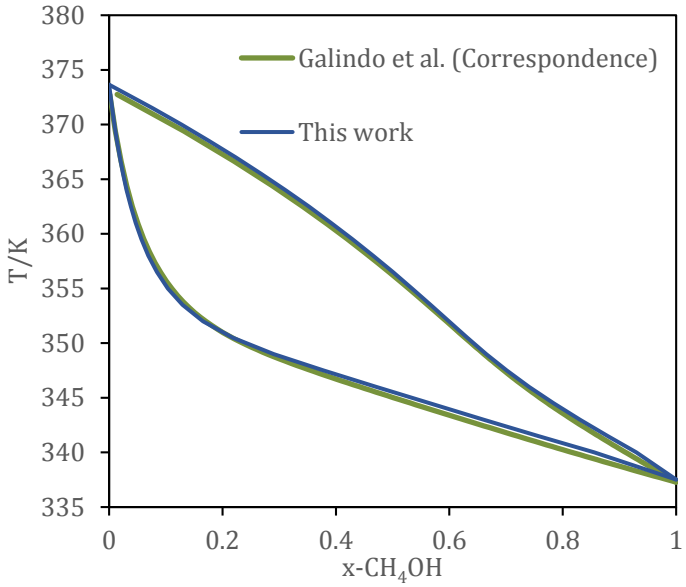

Figure 10: Methanol + water VLE at 1 atm

Both implementations use a non-zero binary interaction parameter (k_{ij}=0.04). The minor discrepancies between the two sets of calculations can be attributed to variations in the degree of precision assigned to code variables.

The good agreement between model predictions and experimental/literature results (including code-to-code comparison with Imperial College London) for each case allowed us to confidently proceed with the extension of the model to mixtures with electrolytes.

4.2. Extension to Electrolyte Solutions

Mean ionic activity coefficients and densities were calculated for various water + salt systems. The salts comprised of combinations of the following 9 cations and 4 anions: Na^+, K^+, Li^+, Rb^+, Cs^+, Mg^{2+}, Ca^{2+}, Sr^{2+}, Ba^{2+}, Cl^-, Br^-, I^-, and F^-.

For each ion-solvent pair, the model has only one adjustable parameter – the cross-dispersion energy parameter between the ion and the solvent ($\varepsilon_{i\text{-}solv}$) . This is the energy well depth in the equation for the Mie potential (2.3), as it pertains to the pair interaction between the ion and the solvent molecule. These parameters were optimized sequentially using experimental data (mean ionic activity coefficients and liquid densities) [39] for sets of salt + water systems – each set consisting of a predetermined "group" of strongly dissociating ions. These groups are illustrated as schematic diagram in Figure 11 – based on a similar scheme presented by Zuber et al. [12].

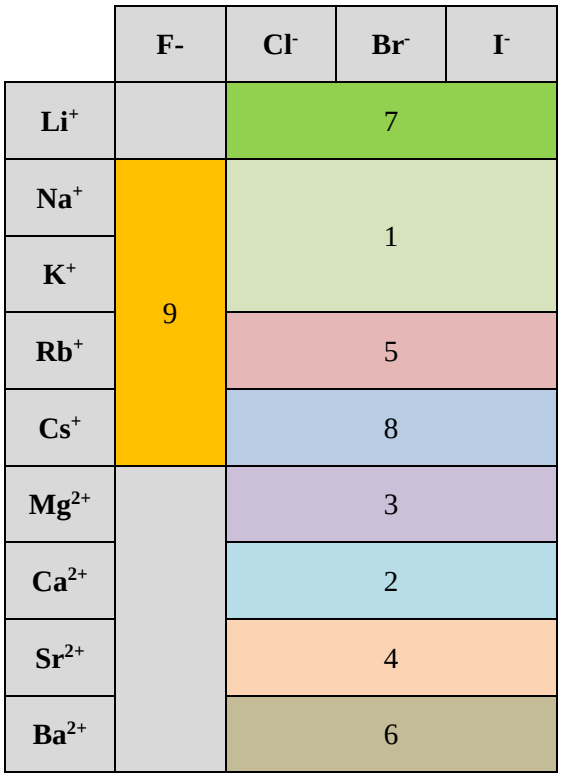

Figure 11: Schematic view of ion groups used in parameter fitting. The numbers correspond to the sequence of parameter optimization i.e. parameters for ions in group 1 were optimized first and so on.

This process yielded the optimized model parameters tabulated in Table 2:

Table 2: Ion-solvent cross dispersion parameters ($\varepsilon_{i\text{-}water}$)

Ion	$\varepsilon_{i\text{-}water}/k_B$ **(K)**
Na^+	157.14
K^+	64.45
Li^+	834.39
Rb^+	73.98
Cs^+	114.27
Mg^{2+}	1766.71
Ca^{2+}	851.59
Sr^{2+}	522.50
Ba^{2+}	335.02
Cl^-	560.92
Br^-	539.08
I^-	511.86
F^-	1052.55

Tables 3 and 4 report the absolute average relative deviation (% AARD) between properties calculated by the model and experimental data [40-43]. These are juxtaposed with the corresponding % AARD data for the model developed by Eriksen et al. [21]. Both models use SAFT-VR Mie to quantify short-range interactions; this engenders a basis for meaningful comparison.

Table 3: % AARD in **liquid density** correlations using the EoS developed in this work and using the model developed by Eriksen et al. [21] at 1 atm for various aqueous electrolytes

Salt	New model			Eriksen et al. [21]		
	% AARD	Temperature Range / K	Max Molality (mol/kg-w)	% AARD	Temperature range / K	Max Molality (mol/kg-w)
NaCl	**2.12**	273.15-373.15	6.01	**5.07**	298-473	5.0
NaBr	**1.51**	273.15-373.15	5.23	**4.36**	283-343	8.3
NaI	**1.15**	283.15-373.15	4.45	**10.10**	298	1.7
NaF	**0.41**	291.15	1.25	**1.02**	297-498	1.0
KCl	**1.78**	273.15-373.15	3.78	**7.03**	298-353	4.0
KBr	**1.63**	273.15-373.15	4.52	**2.91**	283-348	5.8
KI	**1.20**	283.15-373.15	3.24	**3.02**	278-373	1.0
KF	**2.41**	291.15	6.05	**1.69**	297-372	8.9
LiCl	**1.12**	273.15-373.15	10.11	**1.85**	278-343	10.0
LiBr	**0.78**	273.15-373.15	9.42	**1.09**	378-343	10.0
LiI	**0.87**	273.15-373.15	11.21	**2.18**	298-373	4.9
RbCl	**2.14**	273.15-323.15	8.27	**0.76**	298	5.0
RbBr	**1.73**	273.15-323.15	7.39	**4.56**	298-323	6.8
RbI	**1.47**	273.15-323.15	5.76	**3.07**	298-310	0.4
RbF	**1.73**	291.15	4.50	**7.11**	298	0.5
CsCl	**5.93**	298.15-343.34	7.52	-	-	-
CsBr	**4.01**	298.15-343.34	4.19	-	-	-
CsI	**2.75**	298.15-343.34	2.89	-	-	-
CsF	**14.73**	273.15-323.15	4.67	-	-	-
$MgCl_2$	**2.04**	288.15-328.15	5.00	**2.50**	288-372	4.8
$MgBr_2$	**1.34**	273.15-373.15	4.44	**0.74**	298	3.7
MgI_2	**1.13**	273.15-373.15	2.40	-	-	-
$CaCl_2$	**3.06**	288.15-328.15	6.00	**2.59**	288-328	4.0
$CaBr_2$	**2.31**	273.15-373.15	5.00	**1.98**	298	3.4
CaI_2	**1.72**	273.15-373.15	2.27	-	-	-
$SrCl_2$	**2.28**	288.15-328.15	2.50	-	-	-
$SrBr_2$	**2.16**	273.15-373.15	4.04	**1.51**	298	2.4
SrI_2	**1.84**	273.15-373.15	2.40	-	-	-
$BaCl_2$	**1.76**	288.15-328.15	1.5	**2.02**	288-328	1.5
$BaBr_2$	**1.56**	273.15-373.15	2.24	**2.92**	298	1.6
BaI_2	**2.38**	273.15-373.15	3.83	-	-	-

Table 4: % AARD in **mean ionic activity coefficient** correlations of the EoS developed in this work and using the model of Eriksen et al. [21] at 1 atm and 298.15 K for various aqueous electrolytes.

Salt	New model			Eriksen et al. [21]		
	% AARD	Max Molality (mol/kg-w)	Number of Exptl. Data Points	% AARD	Max Molality (mol/kg-w)	Number of Exptl. Data Points
NaCl	**3.39**	6.0	35	**20.43**	6.1	30
NaBr	**3.91**	4.0	19	**7.92**	8.2	47
NaI	**2.54**	4.5	26	**5.01**	3.5	14
NaF	**5.20**	1.0	10	**8.40**	1.0	6
KCl	**2.81**	4.5	20	**11.60**	4.0	80
KBr	**2.76**	4.5	20	**1.73**	5.5	36
KI	**2.63**	3.5	18	**11.73**	4.0	35
KF	**4.46**	4.0	19	**8.02**	4.0	15
LiCl	**11.50**	4.5	19	**16.79**	10.0	48
LiBr	**4.26**	4.5	20	**14.22**	9.0	34
LiI	**7.97**	3.0	17	**10.98**	3.0	33
RbCl	**4.66**	5.0	21	**1.03**	5.0	17
RbBr	**0.99**	5.0	27	**7.68**	5.0	32
RbI	**2.10**	5.0	27	**26.51**	5.0	34
RbF	**4.61**	3.5	24	**4.74**	3.5	14
CsCl	**2.79**	5.0	21	**-**	-	-
CsBr	**2.13**	5.0	21	**-**	-	-
CsI	**4.84**	3.0	17	**-**	-	-
CsF	**3.89**	3.50	24	**-**	-	-
$MgCl_2$	**30.23**	3.0	17	**16.49**	5.9	53
$MgBr_2$	**26.74**	5.0	21	**8.52**	3.0	15
MgI_2	**21.12**	5.0	21	**18.21**	1.6	13
$CaCl_2$	**8.88**	2.5	31	**8.31**	3.0	67
$CaBr_2$	**14.29**	2.0	15	**11.43**	3.0	15
CaI_2	**14.99**	1.8	14	**21.34**	1.8	14
$SrCl_2$	**13.06**	1.3	14	**5.87**	4.0	78
$SrBr_2$	**8.37**	2.0	15	**7.95**	2.0	30
SrI_2	**10.27**	2.0	15	**6.57**	2.0	30
$BaCl_2$	**9.45**	1.8	19	**10.61**	1.4	14
$BaBr_2$	**9.38**	2.0	15	**5.60**	2.3	49 [278-318K]
BaI_2	**10.91**	2.0	15	**7.62**	2.0	30

In general, the new model is equally or more accurate than that of Eriksen et al. [21]. Nevertheless, there is still room for improvement in order to attain the accuracy of models using different formulations for short-range interactions such as the Q-Electrolattice [12] and SAFT2-KMSA [44] equations of state – the latter of which is notable in its accurate representation of the temperature dependence of mean ionic activity coefficients.

Figures 12-17 provide representative results for the liquid density of various 1:1 and 1:2 salts at 298.15 and 373.15 K. Overall, the model provides reasonably accurate correlation of the experimental data for all of the different mixtures examined.

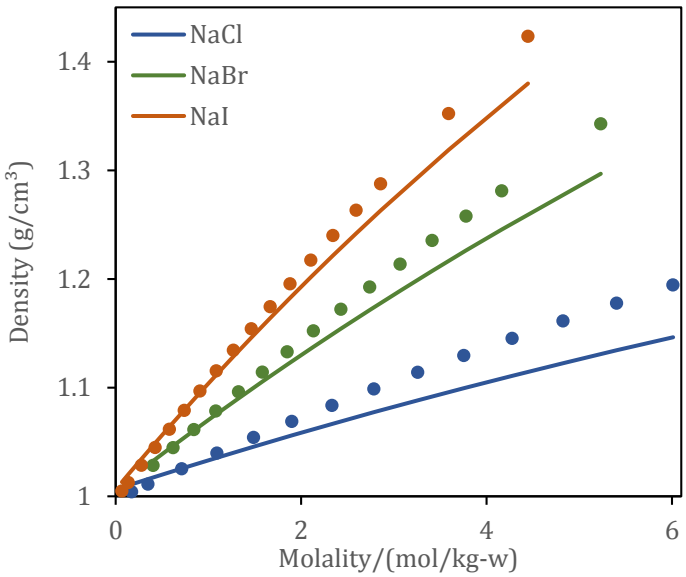

Figure 12: Liquid density of selected sodium salts at 298.15 K and 1 atm. Continuous lines are model correlations and points are experimental data from [43].

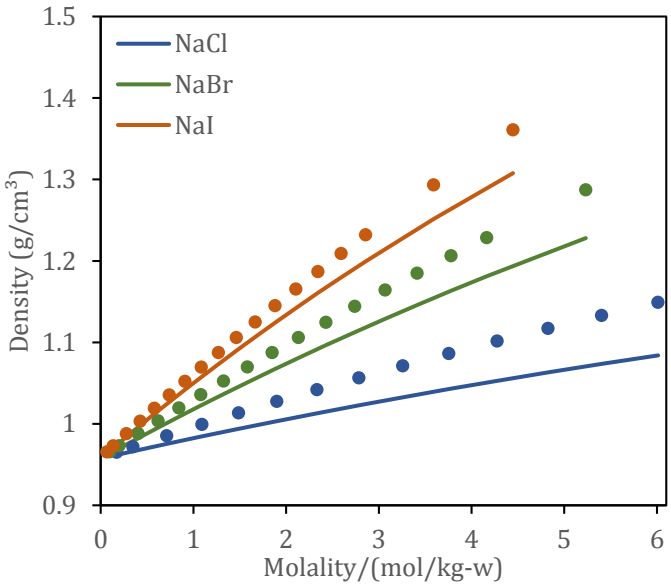

Figure 13: Liquid density of selected sodium salts at 373.15 K and 1 atm. Continuous lines are model correlations and points are experimental data from [43].

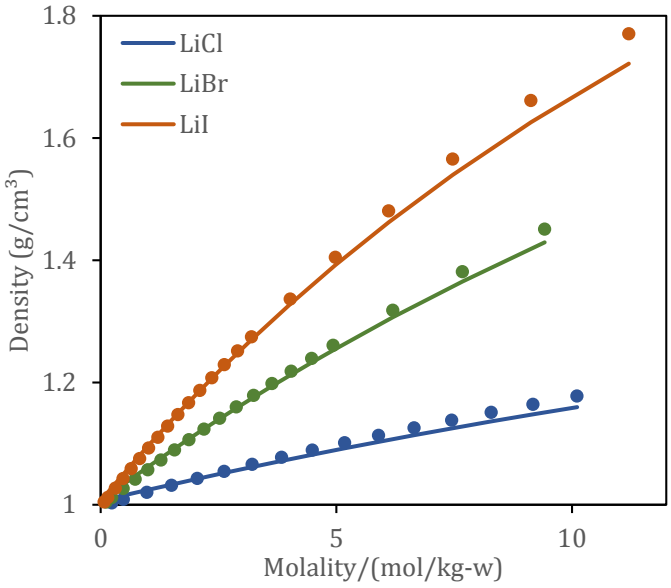

Figure 14: Liquid density of selected lithium salts at 298.15 K and 1 atm. Continuous lines are model correlations and points are experimental data from [43].

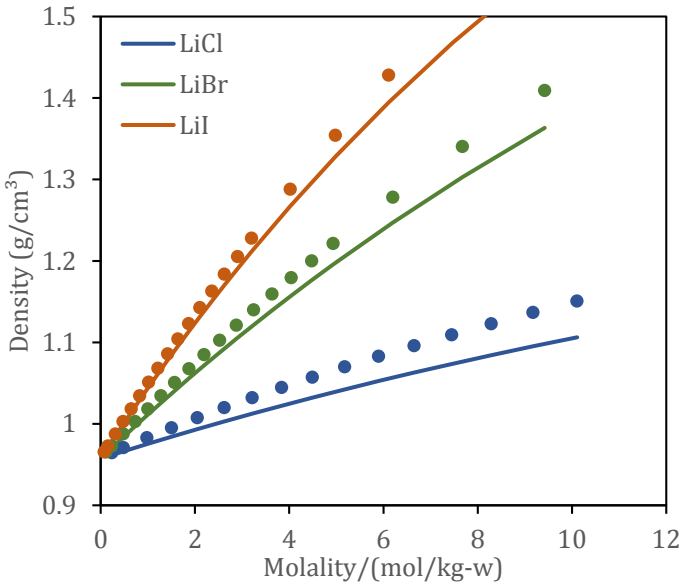

Figure 15: Liquid density of selected lithium salts at 373.15 K and 1 atm. Continuous lines are model correlations and points are experimental data from [43].

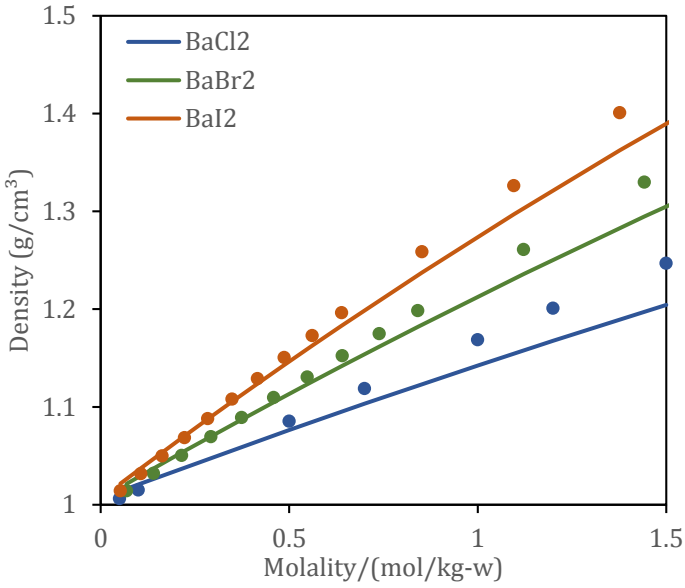

Figure 16: Liquid density of selected barium salts at 298.15 K and 1 atm. Continuous lines are model correlations and points are experimental data from [41, 43].

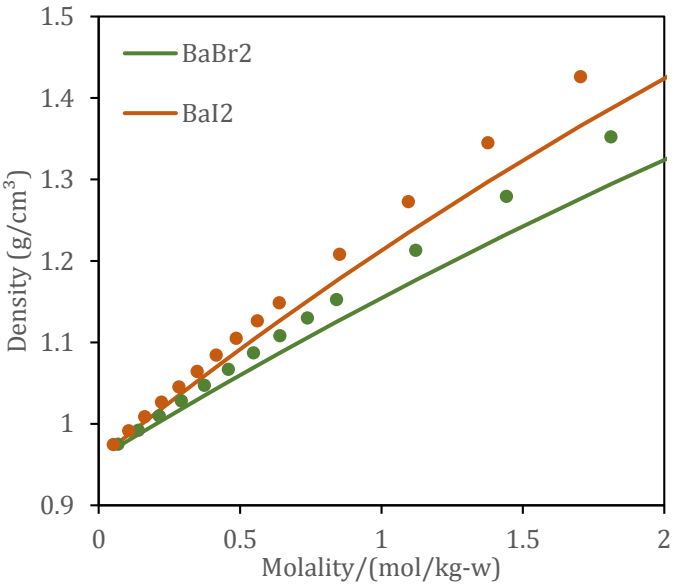

Figure 17: Liquid density of selected barium salts at 373.15 K and 1 atm. Continuous lines are model correlations and points are experimental data from [41, 43].

Clearly, the model systematically under-predicts liquid densities as salt composition increases. This can best be attributed to the use of crystal ionic radii to characterize the σ-parameter for ionic species in the equation of state. Indeed, the value of σ describing a species' Mie potential does not necessarily correspond to its molecular/ionic diameter. It is noteworthy that optimized ionic diameters evaluated for the Q-Electrolattice model are all smaller than the corresponding crystal diameters – allowing for better representation of the densities of concentrated solutions.

This behavior impairs the model's ability to predict liquid densities of mixed ion solutions. Figure 18 shows model predictions of liquid densities for representative mixed ion solutions ($CaCl_2$ + KCl).

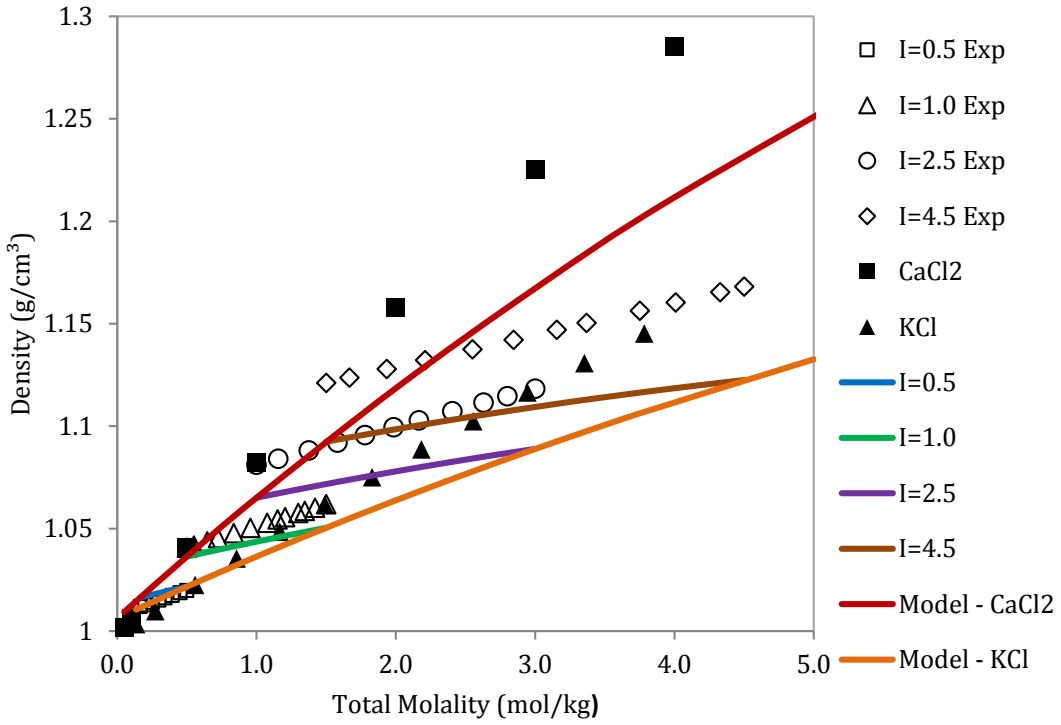

Figure 18: Liquid densities of aqueous solutions at 298.15 K and 1 atm containing $CaCl_2$ + KCl at various ionic strengths. Continuous lines are model predictions and points are experimental data points [41, 43, 45].

Figures 19-28 are plots of the developed model's correlations for the mean ionic activity coefficient for various salt + water systems at 298.15 K and 1 atm.

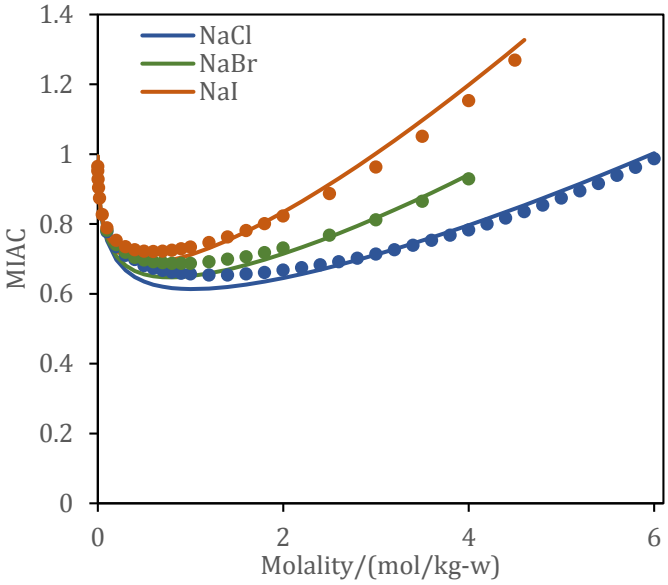

Figure 19: Mean ionic activity coefficients of selected sodium salts at 273.15 K and 1 atm. Continuous lines are model correlations and points are experimental data from [41].

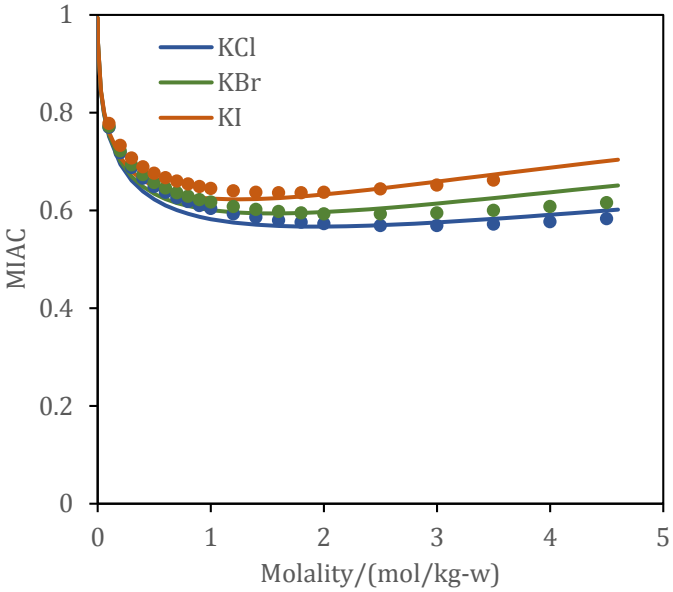

Figure 20: Mean ionic activity coefficients of selected potassium salts at 273.15 K and 1 atm. Continuous lines are model correlations and points are experimental data from [41].

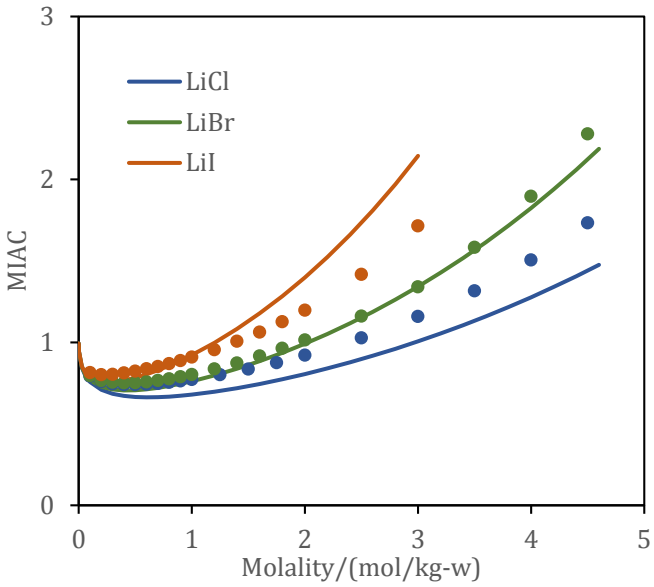

Figure 21: Mean ionic activity coefficients of selected lithium salts at 273.15 K and 1 atm. Continuous lines are model correlations and points are experimental data from [41].

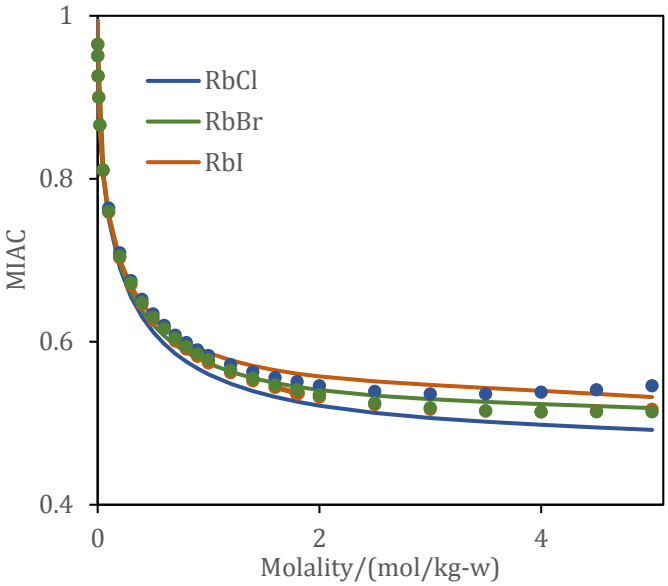

Figure 22: Mean ionic activity coefficients of selected rubidium salts at 273.15 K and 1 atm. Continuous lines are model correlations and points are experimental data from [41].

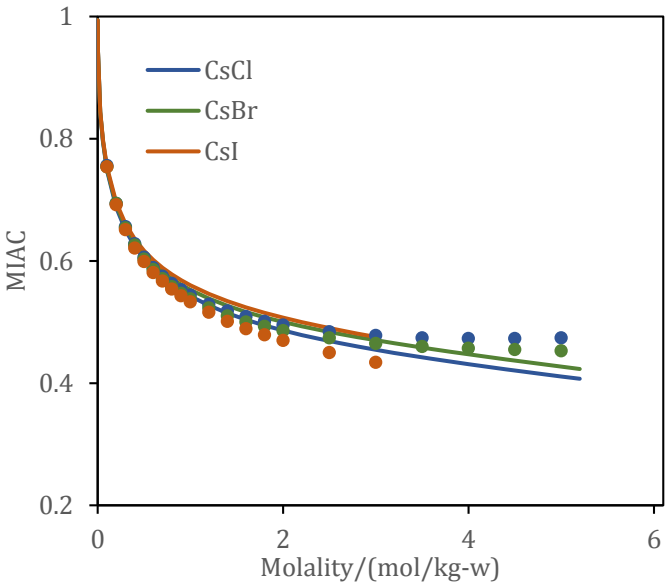

Figure 23: Mean ionic activity coefficients of selected cesium salts at 273.15 K and 1 atm. Continuous lines are model correlations and points are experimental data from [41].

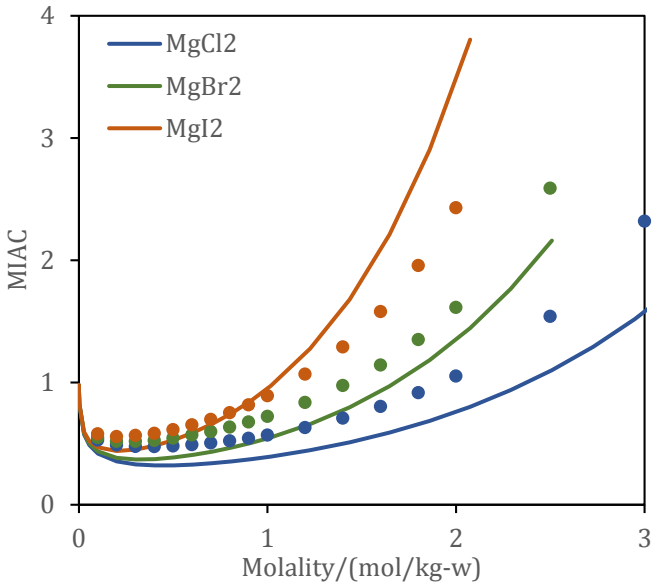

Figure 24: Mean ionic activity coefficients of selected magnesium salts at 273.15 K and 1 atm. Continuous lines are model correlations and points are experimental data from [41].

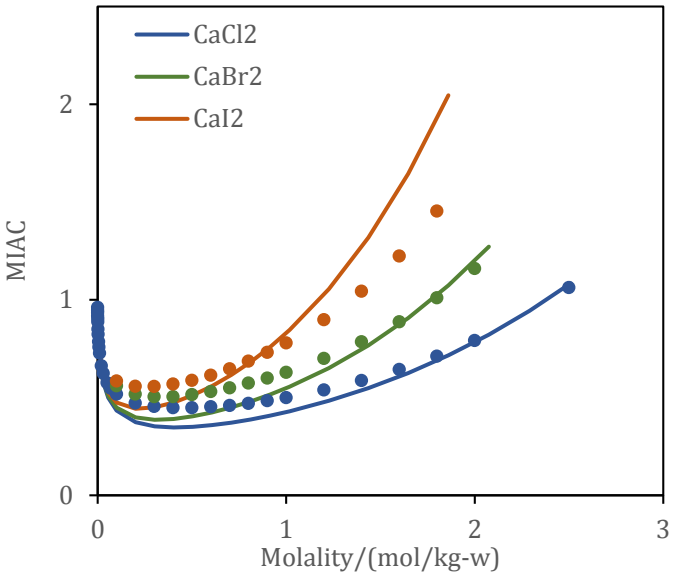

Figure 25: Mean ionic activity coefficients of selected calcium salts at 273.15 K and 1 atm. Continuous lines are model correlations and points are experimental data from [41].

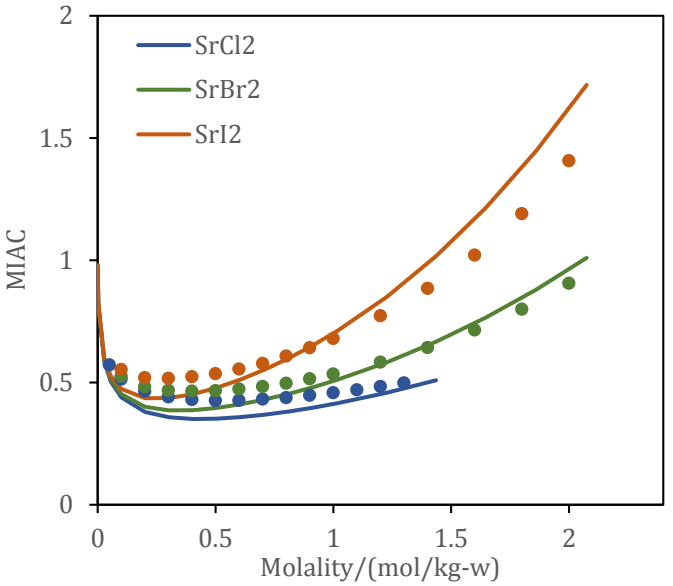

Figure 26: Mean ionic activity coefficients of selected strontium salts at 273.15 K and 1 atm. Continuous lines are model correlations and points are experimental data from [41].

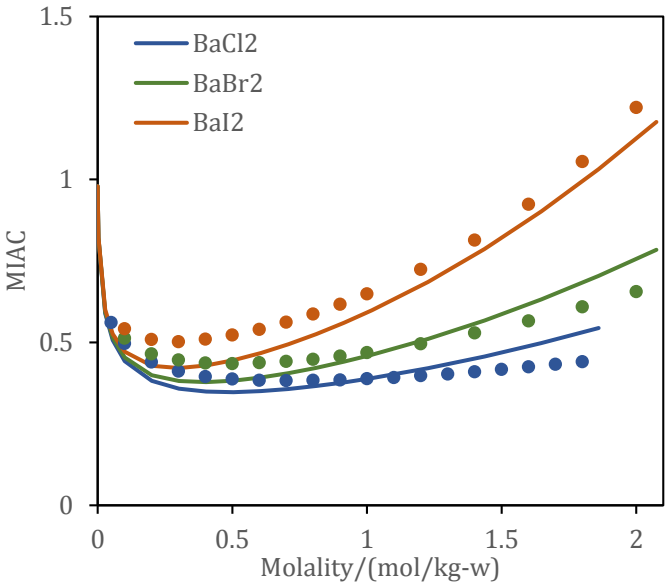

Figure 27: Mean ionic activity coefficients of selected barium salts at 273.15 K and 1 atm. Continuous lines are model correlations and points are experimental data from [41].

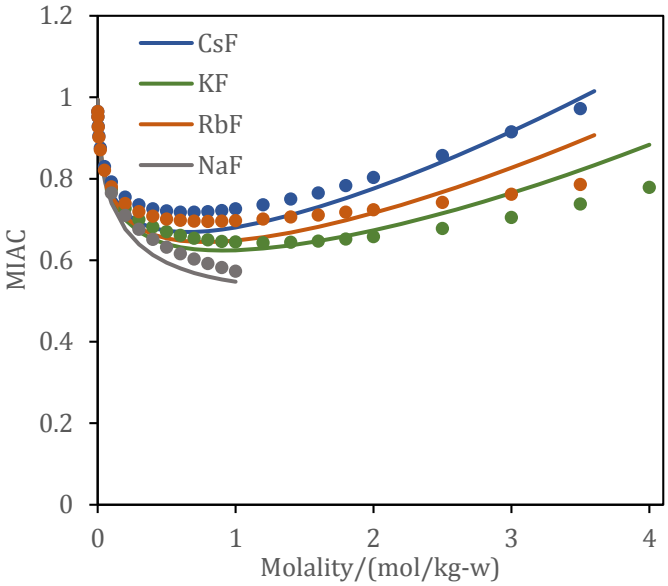

Figure 28: Mean ionic activity coefficients of selected fluorides at 273.15 K and 1 atm. Continuous lines are model correlations and points are experimental data from [40, 42].

The new model is able to capture the qualitative behavior of the compositional dependence of the mean ionic activity coefficient – notably the existence of minimum at relatively low salt compositions. Good quantitative agreement is achieved in most cases. In systems where the model indicates a minimum, it consistently under-predicts its value. This effect is more pronounced in systems containing divalent ions – implying an underlying deficiency in the model's description of electrostatic phenomena.

Figure 29 shows the model's predictions of the mean ionic activity coefficients for aqueous NaCl at various temperatures in the range 273.15-373.15 K.

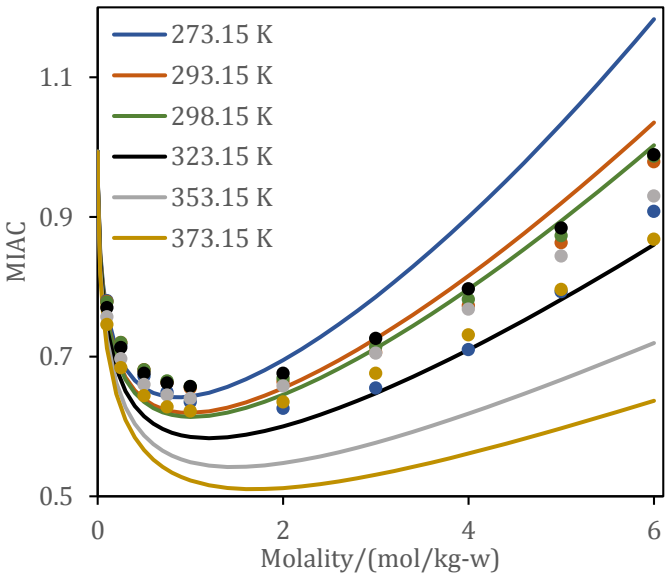

Figure 29: Mean ionic activity coefficient of aqueous NaCl at various temperatures at 1 bar. Continuous lines are model predictions and points are experimental data from [46].

In practice, mean ionic activity coefficients of NaCl increase with temperature from 273 K to approximately 323 K where they reach a maximum, and subsequently decrease with further increases in temperature. The current formulation of the model predicts that the activity coefficients decreases monotonically with the temperature. This deficiency can be attributed both to failure of the model to predict the maximum density of pure water at 4 ^{o}C and consequently aqueous mixture properties in this temperature region, as well as deficiencies in the salt + water model. Further investigation is needed.

Figure 30 shows predictions of osmotic coefficients for selected salt solutions.

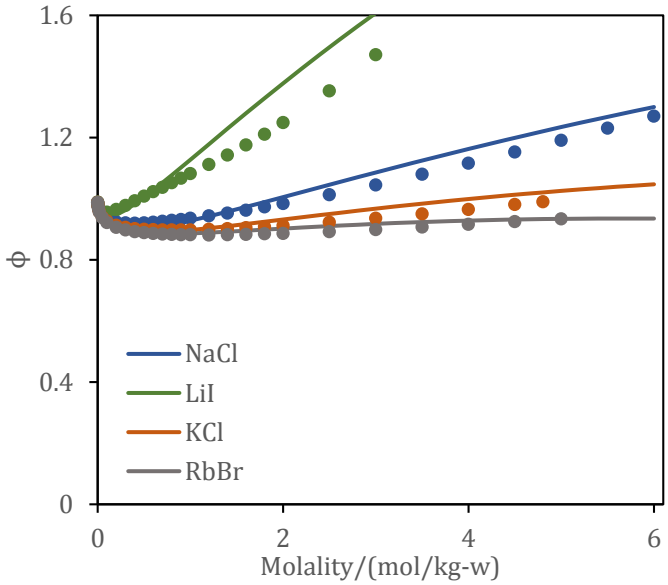

Figure 30: Osmotic coefficients for selected salt solutions at 298.15 K and 1 atm. Continuous lines are model predictions and points are experimental data from [42].

Predictions of osmotic coefficients tend to be more accurate for salt solutions for which the model better correlates activity coefficients. This is understandable, since the two quantities are interdependent as a consequence of the Gibbs-Duhem relation, and are related through the following equation [21]:

$$\ln \gamma_{\pm,m} = \Phi - 1 + \int_0^m \frac{(\Phi - 1)}{\bar{m}} d\bar{m} \tag{4.1}$$

The model performs favorably for vapor pressure calculations for both single and mixed salt solutions. Figure 31 illustrates model predictions of vapor pressures of aqueous NaCl solutions.

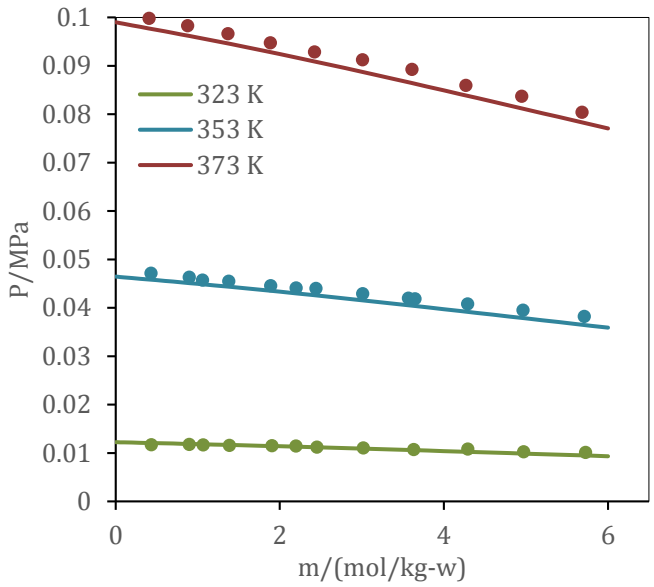

Figure 31: Vapor pressure isotherms for NaCl + water solutions. Continuous lines are model predictions and points are experimental data referenced in [21].

The model's predictions deteriorate somewhat for higher temperatures, but are generally reliable. Figure 32 contains plots of vapor pressures of an aqueous NaBr + KBr solution at two different molality combinations.

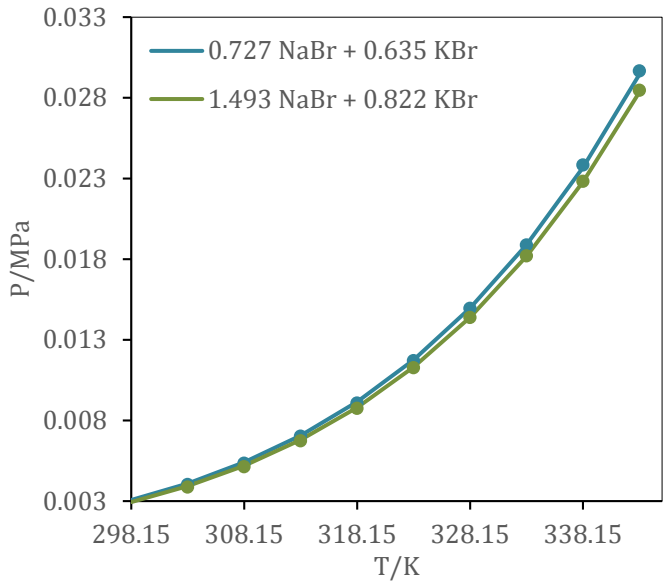

Figure 32: Model predictions for vapor pressures of mixed ion solvents. Continuous lines are model predictions and points are experimental data from [47].

This plot exemplifies how vapor pressure calculations using the equation of state are sensitive to the effect of relatively small perturbations in salt composition. This has a great deal to do with the accuracy of the underlying model for pure water.

5. CONCLUSIONS AND FUTURE WORK

The SAFT-VR Mie EoS has successfully been extended to electrolyte solutions through the inclusion of additional terms to quantify energy contributions of long-range, electrostatic interactions. Specifically, the Debye-Hückel and Born models were used to characterize ion-ion electrostatic interactions and ion solvation effects, respectively. In the developed model, each ionic species has one adjustable parameter which characterizes the cross dispersion energy between the ion and the solvent (which, in this thesis, was always water). This parameter was optimized against experimental data for mean ionic activity coefficients and liquid densities at various temperatures. While the model performs well in comparison to another recent model based on the same SAFT-VR Mie framework for short-range interactions [21], further development of both the mathematical formulation and parameter optimization strategy could make it a more reliable tool for the prediction of thermodynamic properties across wider ranges of salt composition and temperature.

It was noted that the developed model's liquid density calculations deteriorate as salt concentration increases – systematically under-predicting density values. One possible explanation for this is that the crystal diameters of ion species used in this model overstate the Mie potential's "true" σ-value. Alternatively, treating the σ of ionic species as an adjustable parameter (just as is the case for non-ionic species in SAFT-VR Mie) would allow for smaller σ-parameters to emerge, and consequently, a better representation of solution liquid densities.

The model consistently under predicts values of mean ionic activity coefficients at their compositional minimum. This under prediction is more pronounced for systems containing divalent ions – indicating a deficiency in the mathematical description of the systems' electrostatics. One possible source of this deficiency is the model's utilization of a composition and volume independent correlation for the dielectric constant – accounting only for temperature effects. Integrating a more complete treatment of dielectric phenomena with the model may improve its quantitative performance.

A major challenge is capturing the temperature dependence of mean ionic activity coefficients in a predictive fashion (i.e. without resorting to the introduction of empiricisms which dictate the temperature dependence of equation of state parameters). For example, mean ionic activity coefficients of aqueous sodium chloride increase with temperature from 273 K to approximately 323 K where they reach a maximum, and subsequently decrease with further increases in temperature. This implies competing temperature dependent effects. Identifying these effects and incorporating them into the existing model is a multi-scale problem – involving both a mathematical analysis of the model itself and insight from a better understanding of fundamental physical phenomena at the molecular level. One source of deficiency may be the relatively inaccurate model for pure water at low temperatures.

With respect to broadening the applicability of the model to engineering applications, future work should include its extension to mixed solvents. Another useful task would be the implementation of a reactive scheme to model CO_2 dissolution in salt +

hydrocarbon mixtures which accounts for the effect of pH changes on the thermodynamics of such solutions.

REFERENCES

[1] D. P. Tassios, *Applied Chemical Engineering Thermodynamics*, 1st ed. New York: Springer-Verlag Berlin, 1993.

[2] D. Frenkel and B. Smit, *Computational science series : Understanding Molecular Simulation : From Algorithms to Applications (2)*. Amsterdam, US: Academic Press, 2001.

[3] W. G. Chapman, K. Gubbins, C. Joslin, and C. Gray, "Theory and simulation of associating liquid mixtures," *Fluid Phase Equilibria*, vol. 29, 337-346, 1986.

[4] B. Felipe J and V. Lourdes F, "Thermodynamic behaviour of homonuclear and heteronuclear Lennard-Jones chains with association sites from simulation and theory," *Molecular Physics*, vol. 92, 135-150, 1997.

[5] A. Gil-Villegas, A. Galindo, P. J. Whitehead, S. J. Mills, G. Jackson, and A. N. Burgess, "Statistical associating fluid theory for chain molecules with attractive potentials of variable range," *J Chem Phys*, vol. 106, 4168-4186, 1997.

[6] J. Gross and G. Sadowski, "Perturbed-chain SAFT: An equation of state based on a perturbation theory for chain molecules," *Industrial & Engineering Chemistry Research*, vol. 40, 1244-1260, 2001.

[7] T. Lafitte, A. Apostolakou, C. Avendano, A. Galindo, C. S. Adjiman, E. A. Muller, and G. Jackson, "Accurate statistical associating fluid theory for chain molecules formed from Mie segments," *J Chem Phys*, vol. 139, 154504, 2013.

[8] S. I. Sandler, *An Introduction to Applied Statistical Thermodynamics*, 1st ed. Hoboken, NJ: John Wiley & Sons, Inc., 2011.

[9] S. Dufal, T. Lafitte, A. J. Haslam, A. Galindo, G. N. I. Clark, C. Vega, and G. Jackson, "The A in SAFT: developing the contribution of association to the Helmholtz free energy within a Wertheim TPT1 treatment of generic Mie fluids," *Molecular Physics*, vol. 113, 948-984, 2015.

[10] J. M. Prausnitz, R. N. Lichtenthaler, and E. G. d. Azevedo, *Molecular thermodynamics of fluid-phase equilibria*, 3rd ed. / ed. Upper Saddle River, N.J. :: Prentice Hall PTR, 1999.

[11] A. Zuber, R. F. Checoni, R. Mathew, J. P. L. Santos, F. W. Tavares, and M. Castier, "Thermodynamic Properties of 1:1 Salt Aqueous Solutions with the Electrolattice

Equation of State," *Oil & Gas Science and Technology – Revue d'IFP Energies nouvelles,* vol. 68, 255-270, 2013.

[12] A. Zuber, R. F. Checoni, and M. Castier, "Thermodynamic properties of aqueous solutions of single and multiple salts using the Q-electrolattice equation of state," *Fluid Phase Equilibria,* vol. 362, 268-280, 2014.

[13] K. E. Gubbins, "Perturbation theories of the thermodynamics of polar and associating liquids: A historical perspective," *Fluid Phase Equilibria,* vol. 416, 3-17, 2016.

[14] N. F. Carnahan, "Equation of State for Nonattracting Rigid Spheres," *J Chem Phys,* vol. 51, 635, 1969.

[15] M. Michelsen and E. Hendriks, "Physical Properties from Association Models," *Fluid Phase Equilibria,* 165-174, 2000.

[16] K. Thomsen, "Electrolyte Solutions: Thermodynamics, Crystallization, Separation methods," ed: Technical University of Denmark, 2006.

[17] B. Maribo-Mogensen, G. M. Kontogeorgis, and K. Thomsen, "Comparison of the Debye–Hückel and the Mean Spherical Approximation Theories for Electrolyte Solutions," *Industrial & Engineering Chemistry Research,* vol. 51, 5353-5363, 2012.

[18] B. Maribo-Mogensen, G. M. Kontogeorgis, and K. Thomsen, "Modeling of dielectric properties of aqueous salt solutions with an equation of state," *J Phys Chem B,* vol. 117, 10523-33, 2013.

[19] B. Maribo-Mogensen, G. M. Kontogeorgis, and K. Thomsen, "Modeling of dielectric properties of complex fluids with an equation of state," *J Phys Chem B,* vol. 117, 3389-97, 2013.

[20] J. M. A. Schreckenberg, S. Dufal, A. J. Haslam, C. S. Adjiman, G. Jackson, and A. Galindo, "Modelling of the thermodynamic and solvation properties of electrolyte solutions with the statistical associating fluid theory for potentials of variable range," *Molecular Physics,* vol. 112, 2339-2364, 2014.

[21] D. K. Eriksen, G. Lazarou, A. Galindo, G. Jackson, C. S. Adjiman, and A. J. Haslam, "Development of intermolecular potential models for electrolyte solutions using an electrolyte SAFT-VR Mie equation of state," *Molecular Physics,* 1-26, 2016.

[22] A. Zuber, L. Cardozo-Filho, V. F. Cabral, R. F. Checoni, and M. Castier, "An empirical equation for the dielectric constant in aqueous and nonaqueous electrolyte mixtures," *Fluid Phase Equilibria,* vol. 376, 116-123, 2014.

[23] Y.-X. Zuo and W. Fürst, "Prediction of vapor pressure for nonaqueous electrolyte solutions using an electrolyte equation of state," *Fluid Phase Equilibria,* vol. 138, 87-104, 1997.

[24] J. A. Myers, S. I. Sandler, and R. H. Wood, "An Equation of State for Electrolyte Solutions Covering Wide Ranges of Temperature, Pressure, and Composition," *Industrial & Engineering Chemistry Research,* vol. 41, 3282-3297, 2002.

[25] C. Held, L. F. Cameretti, and G. Sadowski, "Modeling aqueous electrolyte solutions: Part 1. Fully dissociated electrolytes," *Fluid Phase Equilibria,* vol. 270, 87-96, 2008.

[26] B. Maribo-Mogensen, K. Thomsen, and G. M. Kontogeorgis, "An electrolyte CPA equation of state for mixed solvent electrolytes," *AIChE Journal,* vol. 61, 2933-2950, 2015.

[27] H. L. Friedman, "Lewis-Randall to McMillan-Mayer conversion for the thermodynamic excess functions of solutions. Part I. Partial free energy coefficients," *Journal of Solution Chemistry,* vol. 1, 387-412, 1972.

[28] K. S. Pitzer, "Thermodynamics of electrolytes. I. Theoretical basis and general equations," *The Journal of Physical Chemistry,* vol. 77, 268-277, 1973.

[29] K. S. Pitzer and G. Mayorga, "Thermodynamics of electrolytes. II. Activity and osmotic coefficients for strong electrolytes with one or both ions univalent," *The Journal of Physical Chemistry,* vol. 77, 2300-2308, 1973.

[30] C.-C. Chen and Y. Song, "Extension of Nonrandom Two-Liquid Segment Activity Coefficient Model for Electrolytes," *Industrial & Engineering Chemistry Research,* vol. 44, 8909-8921, 2005.

[31] G. A. Iglesias-Silva, A. Bonilla-Petriciolet, P. T. Eubank, J. C. Holste, and K. R. Hall, "An algebraic method that includes Gibbs minimization for performing phase equilibrium calculations for any number of components or phases," *Fluid Phase Equilibria,* vol. 210, 229-245, 2003.

[32] R. J. Topliss, D. Dimitrelis, and J. M. Prausnitz, "Computational aspects of a non-cubic equation of state for phase-equilibrium calculations. Effect of density-dependent mixing rules," *Computers & Chemical Engineering,* vol. 12, 483-489, 1988.

[33] A. A. Rashin and B. Honig, "Reevaluation of the Born model of ion hydration," *The Journal of Physical Chemistry,* vol. 89, 5588-5593, 1985.

[34] R. Shannon, "Revised effective ionic radii and systematic studies of interatomic distances in halides and chalcogenides," *Acta Crystallographica Section A,* vol. 32, 751-767, 1976.

[35] A. J. Haslam, A. Galindo, and G. Jackson, "Prediction of binary intermolecular potential parameters for use in modelling fluid mixtures," *Fluid Phase Equilibria,* vol. 266, 105-128, 2008.

[36] M. Castier, R. F. Checoni, and A. Zuber, "Fitting equation of state parameters in parallel computers," *Brazilian Journal of Chemical Engineering*, 2014.

[37] D.R. Burgess, "Thermochemical Data" in NIST Chemistry WebBook, NIST Standard Reference Database Number 69, Eds. P.J. Linstrom and W.G. Mallard, National Institute of Standards and Technology, Gaithersburg MD, 20899, http://webbook.nist.gov.

[38] Wichterle and R. Kobayashi, "Vapor-liquid equilibrium of methane-ethane system at low temperatures and high pressures," *Journal of Chemical & Engineering Data,* pp. 9-12, 1972.

[39] V. M. M. Lobo and J. L. Quaresma, *Handbook of electrolyte solutions. Part B.* Amsterdam ;: Elsevier, 1989.

[40] W. J. Hamer and Y. C. Wu, "Osmotic Coefficients and Mean Activity Coefficients of Uni-univalent Electrolytes in Water at 25°C," *Journal of Physical and Chemical Reference Data,* vol. 1, 1047-1100, 1972.

[41] V. M. M. Lobo and J. L. Quaresma, *Handbook of electrolyte solutions. V.M.M. Lobo*: Amsterdam ; New York : Elsevier, 1989., 1989.

[42] R. A. Robinson and R. H. Stokes, "Tables of osmotic and activity coefficients of electrolytes in aqueous solution at 25[degree] C," *Transactions of the Faraday Society,* vol. 45, 612-624, 1949.

[43] E. W. Washburn, "International Critical Tables of Numerical Data, Physics, Chemistry and Technology (1st Electronic Edition)," ed: Knovel.

[44] H. Jiang, A. Z. Panagiotopoulos, and I. G. Economou, "Modeling of CO 2 solubility in single and mixed electrolyte solutions using statistical associating fluid theory," *Geochimica et Cosmochimica Acta,* vol. 176, 185-197, 2016.

[45] A. Kumar, "Densities and apparent molal volumes of aqueous potassium chloride-calcium chloride mixtures at 298.15 K," *Journal of Chemical & Engineering Data,* vol. 31, 21-23, 1986.

[46] K. S. Pitzer, J. C. Peiper, and R. H. Busey, "Thermodynamic Properties of Aqueous Sodium Chloride Solutions," *Journal of Physical and Chemical Reference Data,* vol. 13, 1-102, 1984.

[47] I. M. Shiah and H.-C. Tseng, "Experimental and theoretical determination of vapor pressures of NaCl+KCl, NaBr+KBr and NaCl+CaCl2 aqueous solutions at 298 to 343 K," *Fluid Phase Equilibria,* vol. 124, 235-249, 1996.

APPENDIX

MODEL PARAMETERS

Component-specific SAFT-VR Mie Parameters [7, 9]

Component	m_s	σ / Å	λ_r	λ_a	(ε / k_b) / K	$(\varepsilon_{AB}^{HB} / k_b)$ / K	K_{AB} / Å^3
Methane	1.0000	3.7412	12.650	6	153.36	-	-
Ethane	1.4373	3.7257	12.400	6	206.12	-	-
n-Hexane	2.1097	4.4230	17.203	6	354.38	-	-
Water	1.0000	3.0555	35.823	6	418.00	1600.0	496.66

Parameters for the Evaluation of the Pure Solvent Dielectric Constant [22]

Parameters for Equation (2.41) [23]

Solvent	d_1	d_2	d_3	d_4	d_5
Water	-19.2905	29814.5	-0.019678	1.3189E-4	-3.1144E-7

Ion-specific Parameters [21]

Ion	σ_{ii} / Å	σ_{ii}^{Born} / Å	λ_r	λ_a	I_i / eV	$\alpha_{0,i}$ / 10^{-24} cm^3
Na^+	2.3200	3.3600	12	6	47.2864	0.1790
K^+	3.0400	4.3440	12	6	31.6300	0.8300
Li^+	1.8000	2.6320	12	6	75.6400	0.0290
Rb^+	3.3200	4.6220	12	6	27.2895	1.4000
Cs^+	3.6200	5.0280	12	6	23.1575	2.4200
Mg^{2+}	1.7200	2.9100	12	6	80.1483	0.0940
Ca^{2+}	2.2800	3.7240	12	6	50.9131	0.4700
Sr^{2+}	2.6400	4.1080	12	6	42.8900	0.8600
Ba^{2+}	2.9800	4.2380	12	6	35.8400	1.5500
Cl^-	3.3400	3.8740	12	6	3.6127	3.6600
Br^-	3.6400	4.1740	12	6	3.3636	4.7700
I^-	4.1200	4.6860	12	6	3.0590	7.1000
F^-	2.3800	2.8460	12	6	3.4012	1.0400